TESINA DE ESPECIALIDAD
Escuela Técnica Superior de Ingenieros de Caminos, Canales y Puertos

Geosynthetic reinforced fill to bridge voids

By

Carlos Gómez Pizá

Department of Civil Engineering
Imperial College London

June 2009

Supervisors:
Dr. Lidija Zdravkovic (Imperial College)
Dr. Antonio Gens (Universitat Politècnica de Catalunya)

Abstract

Title: Geosynthetic reinforced fill to bridge voids
Author: Carlos Gómez Pizá
Supervisors: Dr. Lidija Zdravkovic (Imperial College)
Dr. Antonio Gens (Universitat Politècnica de Catalunya)

Geosynthetic reinforced fills are commonly used in areas which have a high risk of sinkhole formation. Brownfield sites are an important example of such areas, since they are commonly in-filled with material placed in an unengineered manner, resulting in poorly compacted terrains with high risk of collapse. Deep foundations are usually not a cost effective solution for low-rise structures, and therefore the construction of a geosynthetic reinforced fill layer capable of bridging any potential void that could form in the underlying soil is one of the alternative recommended solutions.

Soil arching has been identified in previous studies as the load transfer mechanism by which the overlying fill layer can avoid its collapse when a void forms beneath the geosynthetic layer. This study investigates the mobilisation of the soil arching mechanism with respect to the shape and size of the void. In particular, as previous studies consider the formation of a void with vertical boundaries, this study is based on the case in which the vertical boundaries of the void have a certain inclination.

A parametric numerical study based in a finite element model was performed for this purpose, in which the shape and size of the void, the inclination of its vertical boundaries, the construction sequence, the angle of shearing resistance and the properties controlling the compaction of the fill were varied. The results were then compared with two existing arching theories developed by Terzaghi (1943) and Hewlett and Randolph (1988). It is found that Terzaghi´s approach is more generally applicable although Hewlett and Randolph`s is also suitable in some cases and predicts more accurate results than for the vertical boundaries case. It was also seen that the angle of shearing resistance and the compaction properties such as the soil suction in the fill are important designing parameters for these structures.

Resumen

Título: Rellenos reforzados con geosintéticos para salvar vacíos
Autor: Carlos Gómez Pizá
Tutores: Dr. Lidija Zdravkovic (Imperial College)
Dr. Antonio Gens (Universitat Politècnica de Catalunya)

Los rellenos reforzados con geosintéticos son usados frecuentemente en áreas que tienen un alto riesgo de formación de vacios o cavidades. Las áreas industriales abandonadas son un ejemplo importante de este tipo de terrenos, ya que frecuentemente son rellenadas con material colocado de manera incorrecta, resultando en un terreno poco compacto y con un alto riesgo de colapso. El uso de cimentaciones profundas no suele ser una solución económica para edificios de poca altura, y por lo tanto la construcción de un relleno reforzado con geosintéticos capaz de resistir el colapso ante cualquier vacio o cavidad que se pueda formar en el suelo es una de las soluciones alternativas recomendadas.

En estudios previos se ha comprobado que el efecto de arqueo es el mecanismo de transferencia de carga por el cual se puede evitar el colapso del relleno superior cuando un vacío se forma bajo el geosintético. Este trabajo investiga los efectos de la forma y tamaño del vacío formado en el mecanismo de arqueo del relleno. Concretamente, puesto que estudios previos consideraban la formación de un vacío de contornos verticales, este estudio se basa en el caso en el que los lados verticales del vacío tienen una cierta inclinación.

Con este propósito, se realizó un estudio numérico basado en un modelo de elementos finitos, en el que se variaron la forma y tamaño del vacío, la inclinación de los contornos verticales, la secuencia de construcción, el ángulo de fricción y las propiedades que controlan la compactación del relleno. Los resultados se compararon con dos teorías de arqueo del suelo desarrolladas por Terzaghi (1943) y Hewlett & Randolph (1988). Se comprobó que la teoría de Terzaghi es más aplicable en general aunque la teoría de Hewlett & Randolph también es adecuada en algunos casos y predice resultados más precisos que para el caso de la formación de un vacío de contornos verticales. También se comprobó que el ángulo de fricción del relleno y las propiedades de compactación como la presión de succión son importantes parámetros de diseño para este tipo de estructuras.

Contents

Notation

b	Width of pile cap
c'	Soil cohesion
d	Maximum vertical deflection of the geosynthetic spanning the void
D	Void width
d_s	Maximum vertical deflection at the surface of the soil layer
e	Void ratio
E	Young's modulus
H	Height of granular fill
H_c	Height or arching fill above void
J	Tensile modulus of geosynthetic
K	Stress ratio (= σ'_h / σ'_v)
K_0	Coefficient of earth pressure at rest
K_a	Coefficient of active earth pressure
K_p	Coefficient of passive earth pressure
K_w	Handy's lateral earth pressure coefficient
r	Radius of arc
s	Pile spacing
t	Thickness of geosynthetic
T	Tensile force in the geosynthetic
T_{ult}	Ultimate tensile strength of the geosynthetic
z	Depth below the surface of the soil layer
u	Pore water pressure
w_s	Surcharge applied at the surface of the soil layer
γ	Unit weight of the soil layer
φ'	Angle of shearing resistance

$\boldsymbol{\mu}$	Poisson’s ratio
$\boldsymbol{\nu}$	Angle of dilation
$\boldsymbol{\sigma_h}$	Horizontal stress
$\boldsymbol{\sigma_v}$	Vertical stress
$\boldsymbol{\sigma_R}$	Radial stress
$\boldsymbol{\sigma_\Theta}$	Tangential stress

Chapter 1: Introduction

In some particular terrains, such as those in some brownfield sites, in mining areas or in karstic terrains there is a high risk of soil collapse within these materials. This may lead to the formation of sinkholes or voids, which could propagate to the ground surface. The foundations of any structures situated immediately above would clearly be affected. This problem is especially important because the housing construction around the world is forced into the brownfield sites. The problem with the redevelopment of brownfield sites is that many of them have experienced little or no compaction, and therefore they can experience ground movements when loaded, or if there are changes in the ground water table.

Figure 1.1: A 23m deep sinkhole caused by a collapsed mineshaft in Cornwall (The Times, Monday 22 June 1992)

Poorly compacted brownfield sites is one of the most important examples of terrains which susceptible to this problem, but there are many other circumstances in which a localised ground subsidence or sinkhole can develop. A common reason in the UK is the existence of abandoned mines which can eventually collapse (Kempton, 1992), as shown in Figure 1.1. This is quite common since usually the mines are not designed to last for a long period of time, and because it is often difficult to know the exact location of abandoned mines. The presence of soluble rocks such as gypsum or limestone is another indicator of a risk of sinkhole formation. In these cases, a groundwater flow could dissolve the rocks forming cavities underground.

Figure 1.3 shows an example of a case in which the weathering of the limestone lead to the formation of a remarkably large 18m wide sinkhole. Usually the sinkholes which occur are considerably smaller than this one.

Another reason for the formation of sinkholes was noted by Agaiby and Jones (1996). They noted that the presence of dry or partially saturated cemented soils can lead to large volumetric changes if they lose their cementation upon wetting. A possible solution for when there are such problems in the foundation soil would be the use of deep foundations, but these are generally not economically viable for low-rise construction projects. A more economically suitable solution could be the use of geosynthetics to construct a reinforced fill layer capable of reducing the surface deformations if any void should form in the terrain underneath. If a void should form beneath the geosynthetic, the geosynthetic layer would prevent the overlying fill from falling into the void. The geosynthetic also provides a greater strength since the interaction between the fill and the geosynthetic restrains the movement within the fill. Figure 1.2 shows a sketch of a geosynthetic reinforced fill.

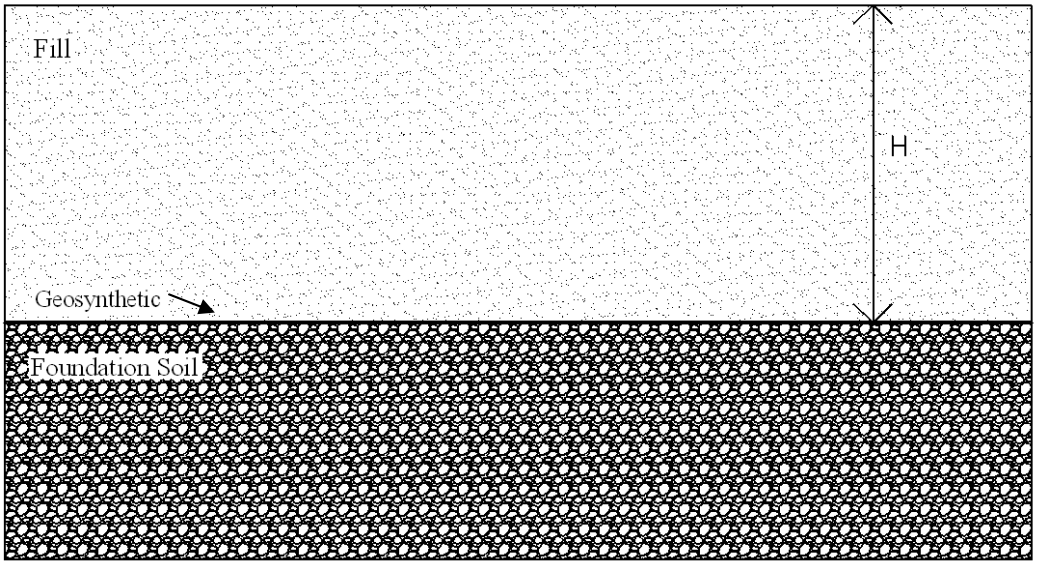

Figure 1.2: Sketch of a geosynthetic reinforced load transfer platform

Geosynthetic reinforced fills have been used in a number of road and railway construction projects, usually located in areas of mining activity or with presence of karstic materials.

The term geosynthetic is typically used for a wide range of products such as geotextiles, geogrids or geocomposites. Their main feature is that at least one of their components is made from a synthetic or natural polymer. For reinforced soil fills the geogrids are the most commonly used.

Figure 1.3: An 18m wide circular sinkhole formed in a limestone area in Missouri, U.S. geological survey (2007)

The reinforced fill layer is based on creating some load transfer mechanism capable of transferring load to the surrounding ground, and hence reducing the pressure at the level of the geosynthetic and the potential damage to the structures on top. Soil arching is the principal mechanism by which the geosynthetic reinforced fill layer can resist collapse when a void forms underneath. Arching is a phenomenon which occurs when one part of a mass of soil moves while the other stays stationary. The friction and shear forces developed in the boundaries between these two masses of soils reduce the total pressure acting on the moving part.

There are some arching theories available in the literature which could be applicable to this case. These theories are analytical means of quantifying the stress state in the soil when there is no vertical support beneath the reinforcement, and they are reviewed in chapter 2. The soil

arching effect is also reviewed with more depth in chapter 2.

It is important to notice that the proposed solution of using a geosynthetic reinforced fill is not intended to be a permanent solution if a void should form beneath it. The intention is simply to maintain the serviceability of the structure until some other remediation measures can be applied, such as excavation, pressure grouting or piling around them. It is not proposed as solution for the cases in which extremely large sinkholes, as the one shown in figure 1.3, should form.

In general it is very difficult to predict the formation of a sinkhole on any particular location, and even more so to predict its size and shape. Therefore we can only determine the areas which have a higher risk of sinkhole formation, a number of examples of such areas have been described previously, and within those areas determine the likely size and shape of the void, usually based on historical knowledge of the ground behavior in that area (Kempton, 1992). The design scenario of this study will therefore be the worst possible case for the formation of a void, which is directly beneath the geosynthetic layer of the load transfer platform.

Objectives

The objectives of the project are:

- To understand the problem through literature survey and model a plan for future work
- As existing arching theories and a previous work by Potts (2007) consider voids with completely vertical sides, the first objective was to investigate the effects that the shape of the void boundary can have on the formation of a soil arch. Two different cases will be considered: the cases in which the void boundary has an inclination of 45º and 60º.
- To analyse the effects of the shape of the void boundary on the vertical stress distribution in the fill and on the deflections of the geosynthetic.
- Analysing the effects of the angle of shearing resistance of the fill.
- To analyse the effects of the angle of the compaction properties of the fill (suction).
- All of the results obtained are to be interpreted and compared with two existing arching theories.

In order to achieve these objectives the first step was to do a literature review describing the phenomenon of soil arching in load transfer platforms as well as the potentially applicable exiting arching theories. A previous study done by Potts (2007) considered the formation of a vertical sides void beneath a geosynthetic reinforced load transfer platform. Due to the similarity with the case of study of this project this work is described with detail in chapter 2. The work done by Mifsud, who analysed a very similar case as Potts, is also reviewed in this chapter.

After the literature review, a numerical study was performed. The finite element method is established as the best strategy for modelling the behaviour of the load transfer platform, for a

number of reasons which are explained in chapter 3. This method is implemented using the Imperial College Finite Element Program (ICFEP), Potts & Zdravkovic (1999).

The results from the numerical analyses performed are shown and discussed in chapter 4. Finally, the conclusions are summarised in the chapter 5. The main results from the finite element analysis are shown in the appendix.

Chapter 2: Literature Review

The behaviour of a load transfer platform such as the geosynthetic reinforced fill embankment analysed in this project is based on the soil arching phenomenon preventing the collapse into a void formed in a potentially collapsible foundation soil. Hence the main objective of this chapter is to analyse this phenomenon and the most appropriate existing arching theories which attempt to predict the behaviour of the fill material above a void.

Potts (2007) analysed the arching behaviour in a geosynthetic reinforced fill above a void with vertical boundaries. The main objective of this project is to enhance this work further, by investigating the fill behaviour above a void with inclined boundaries. Hence this work is also reviewed in this chapter. This chapter also contains literature review on the effects of the compaction properties of the fill, and on the effects of the angle of shearing resistance.

2.1 Soil arching

Arching is a phenomena which occurs when one part of the support of a soil mass yields while the remainder stays in its place. This movement within the soil is opposed by friction or shear forces along the boundaries of the moving and the stationary mass. As a consequence, the total pressure acting on the stationary mass increases by the same amount by which the total pressure decreases in the moving part. This transfer of part of the weight above the yielding strip onto the adjoining masses constitutes the arching effect, and the soil is said to arch over the yielding part of the soil mass.

Arching is therefore a highly desirable phenomenon in a geosynthetic reinforced layer since it reduces the stresses and strains at the level of the geosynthetic reinforcement, as well as reducing the settlements on the surface of the fill layer.

Of the existing arching theories there are two which could be applicable to the case of study. The first one is the Terzaghi's classical arching theory, which is the base of many current design methods. The second theory is Hewlett & Randolph's formulation, which is based on the analysis of a reinforced piled embankment. Both of them are reviewed in the following sections.

2.2 Terzaghi's Arching Theory.

Terzaghi assumes that the soil mass is drained, homogeneous and isotropic, which we know it is difficult to have in practice. It is also assumed that there is no dilation when the soil is shearing. According to Giroud *et al* (1990) if the soil was dilatant the horizontal stresses in the soil would be higher and the transfer of load within the fill would be enhanced. Since most fills should be placed with some compaction it might be reasonable to expect the fill to dilate to some extent. There are some other limitations to this theory, which will be discussed as they are presented.

The shape of the settlement through and the shape of the boundary surface between the stationary and the yielding parts cannot be determined exactly using this theory. Once the sliding part of the soil mass starts to move downwards, a shear failure occurs along a surface which rises vertically from the edges of the void. The settlement trough which forms at the fill surface when the failure occurs is always wider than the void. Therefore the sliding surface is

not completely vertical, although Terzaghi does not give the exact equations. However experiments have been done and it is found that the width of the settlement trough is always greater than that of the void. These experiments suggest that the average slope of the shear surface decreases from almost 90º for low values of H/D to values approaching 45º + φ'/2 for very high values of H/D. An approximate sketch of the shape of the shear surfaces is shown in Figure 2.1.

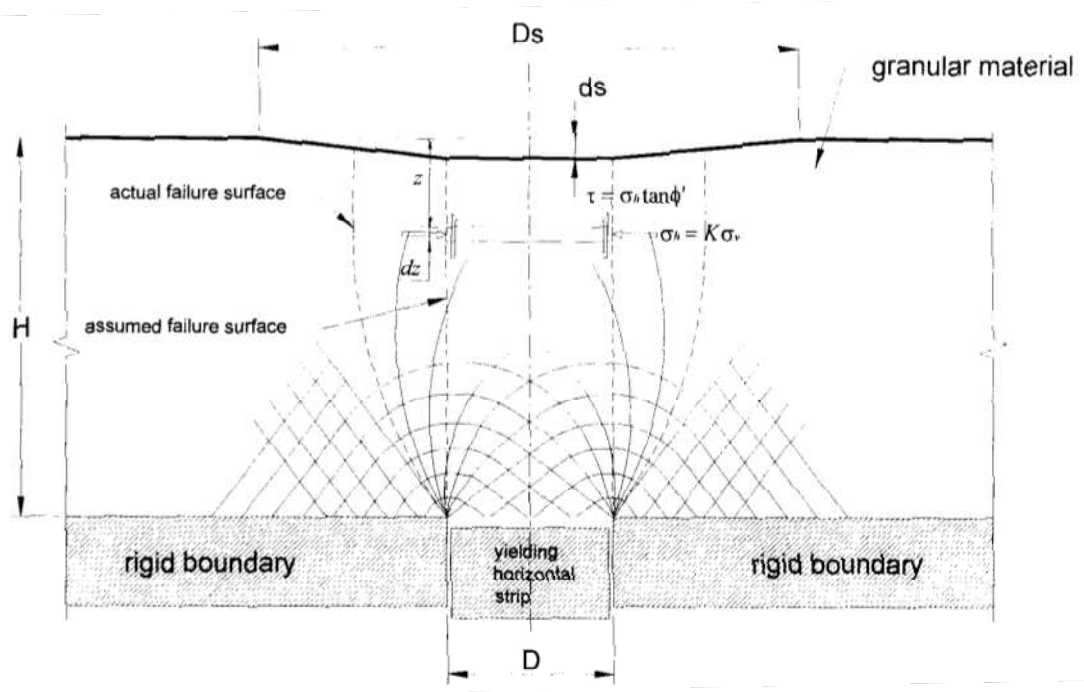

Figure 2.1: Sketch of the shear surfaces formed in a fill above a void (from Mifsud, 2005)

In order to derive Terzaghi´s arching equation we assume that the sliding surfaces are completely vertical and rise from the edges of the void. We know this is not completely true, although it is a good approximation. The derivation is done for the case of an infinitely long longitudinal void.

If we consider a slice of the yielding soil mass, with a unit weight γ, a cohesion c', an angle of internal resistance φ' and a stress ratio K, we can resolve forces in the vertical direction. The strip weighs γ Ddz per unit length perpendicular to the plane of the drawing, and this weight is opposed by friction along the sliding surfaces:

$$\gamma\, D dz + D\,\sigma_v = D(\sigma_v + d\,\sigma_v) + 2cdz + 2K\,\sigma_v \tan\varphi' dz \tag{2.1}$$

This can then be simplified to the following differential equation:

$$\frac{d\sigma_v}{dz} + \frac{2K\tan\varphi'}{D}\sigma_v = \gamma - \frac{2c}{D} \tag{2.2}$$

To solve this equation we can use the condition that $\sigma_v = w_s$ at z = 0, obtaining the following expression for the vertical stress:

$$\sigma_v = \frac{D(\gamma - \frac{2c}{D})}{2K\tan\varphi'}\left(1 - e^{\frac{-2Kz}{D}\tan\varphi'}\right) + w_s e^{\frac{-2Kz}{D}\tan\varphi'} \tag{2.3}$$

2.2.1 Influence of the stress ratio K

The ratio of horizontal to vertical stress, K, is the variable in Terzaghi´s equation with more uncertainty. The correct value to use should be the value of K along the shear surface. We should be expecting high values of K, since the soil in this surface will have experienced some significant disturbance, and it is trying to shed vertical load.

The problem of identifying the suitable value of K to use in Terzaghi´s equation has been addressed by several authors. We could first think of using the at-rest lateral earth pressure coefficient Ko. Handy (1985) proposed an alternative stress ratio K_w, given by the following expression:

$$K_w = 1.06(\cos^2\theta + K_a \sin^2 \theta) \qquad (2.4)$$

Where $\theta = 45^o + \varphi'/2$ and K_a is the Rankine active lateral earth pressure. Therefore this proposed value for the stress ratio only depends on the angle of shearing resistance φ'. This expression proposed by Handy was found empirically.

Another alternative was proposed by Giroud (1990) some years later, which was also found empirically. Giroud found that whenever the angle of shearing resistance φ' is greater than 25º, which would be in many cases, the following expression may be used:

$$K = 0.25/\tan \varphi' \qquad (2.5)$$

Potts and Zdravkovic (2007) performed a numerical analysis using the finite element approach, in which the values of these three proposed values of the stress ratio were compared with the results from a numerical analysis considering infinitely long voids and circular voids. This analysis was also done using the Imperial College Finite Element Program. The analysis was done with the same set of material parameters which will be used in chapter 4, which are summarized in table 2.1. In Figure 2.2 these three stress ratios are compared with the results from the finite element analysis.

These results show that there is some scatter in the values of K computed with the numerical analysis and that the values of K computed using the available formulation in the literature produce very low values for all void widths.

These three methods (K_w, K_0 and $K=0.25/\tan\varphi$) for evaluating the stress ratio significantly overpredict the vertical stresses at the level of the reinforcements. For a circular void and with the same set of parameters, Figure 2.3 shows the vertical stresses for different void widths computed using these three methods, as well as the results from the finite element analysis (labeled as ICFEP). The vertical stresses using a value of K=1.0 in Terzaghi's equation are also plotted.

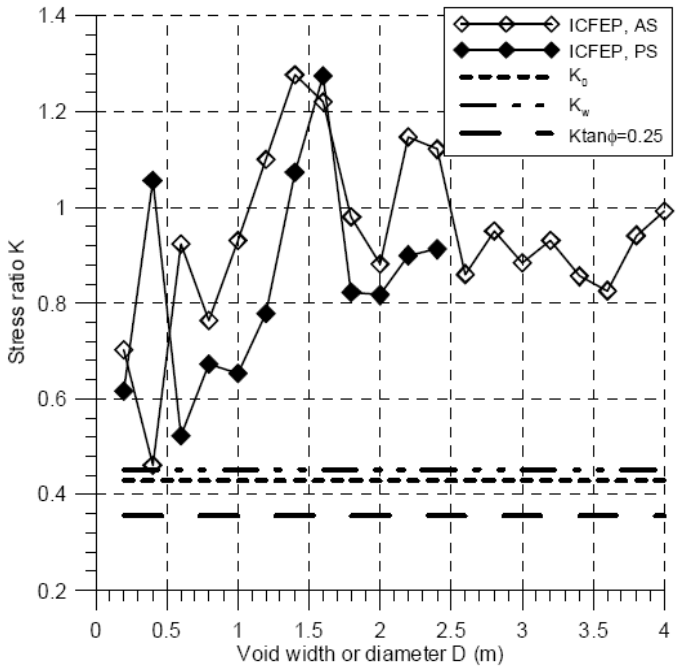

Figure 2.2: Comparison of stress ratios along the shear surfaces computed with a finite element analysis with those available in the literature (from Potts,2007)

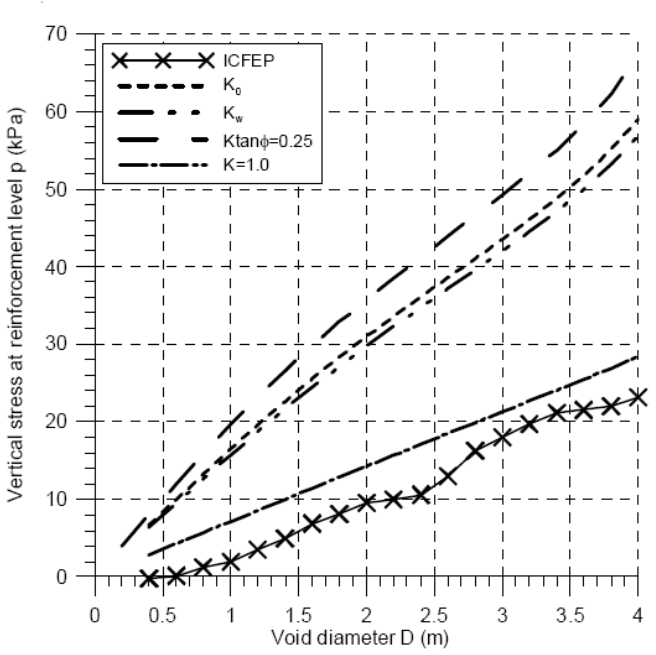

Figure 2.3: Comparison of the vertical stresses at the level of the reinforcement above infinitely long voids computed with Terzaghi's equation using different values of K (from Potts,2007)

Potts and Zdravkovic (2007) propose to use the value of K=1.0 in Terzaghi's equation. Figure 2.3 shows that using this value of K the vertical stresses are slightly overpredicted according to the numerical analysis, but is still more appropriate than the other methods available in the literature.

2.3 Piled embankments

The case of a piled reinforced embankment with a geosynthetic material spanning over the pile caps has been analysed in depth by several authors. The principal problem is to determine how much load is transferred from the embankment to the piles. Figure 2.4 shows a section of a typical piled reinforced embankment.

Potts (2007) noted that there are similarities between this case and the case of a geosynthetic reinforced fill above a void. The main similarity is that in both cases we have portions of much weaker support (voids in the case analysed in this project and embankment fill in the case of a piled embankment) with a geosynthetic layer above.

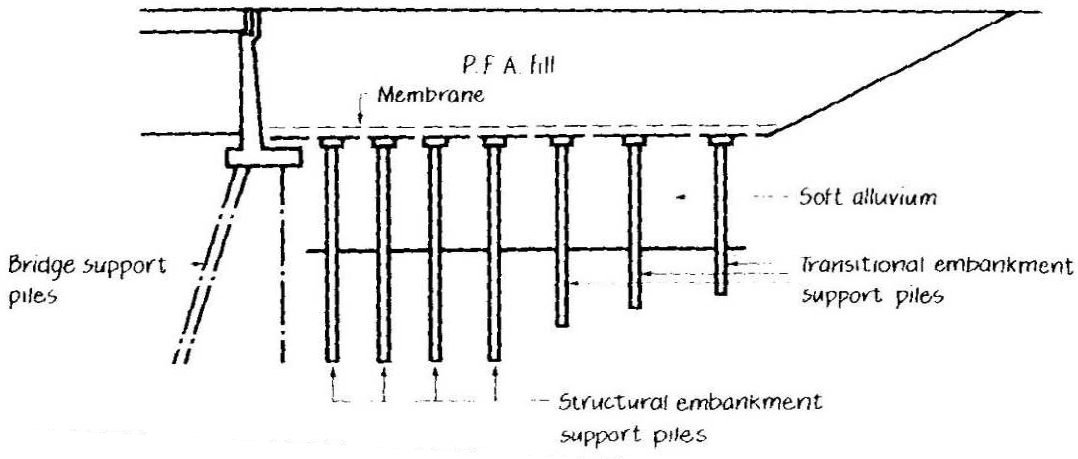

Figure 2.4: Sketch of a typical piled embankment (from Hewlett & Randolph, 1988)

Of all of the methods available in the literature for such a case, Potts (2007) noted that all the previous analyses by Horgan & Sarsby (2002), Russell & Pierpoint (1997) and Love & Milligan (2003) suggested that Hewlett & Randolph's arching theory was the most appropriate. Therefore, this arching theory will be described in the following section.

2.3.1 Hewlett & Randolph's Formulation

Hewlett & Randolph (1988) analysed the arching action of a granular drained embankment fill overlying a rectangular grid of pile caps. Based on laboratory tests they derived general expressions giving the proportion of the weight of the embankment carried directly by the pile caps, in terms of the pile cap size and its centreline spacing, the height of the embankment and the friction angle of the granular fill.

Guided by the mechanisms observed on scale model tests on dry and moist sand they considered the stability of an arched region of sand, as shown in Figure 2.5. The sand within the arcs is in yield condition, whilst the fill above is considered to be at rest. These arches of sand shed the load of the embankment onto the pile caps, hence reducing the load on the subsoil. Within each arch the minor principal stress is in the radial direction and the major principal stress is in the tangential direction. Hewlett and Randolph (1998) noted that there is an analogy in terms of the action of these arches of sand with the masonry arches found in cathedrals.

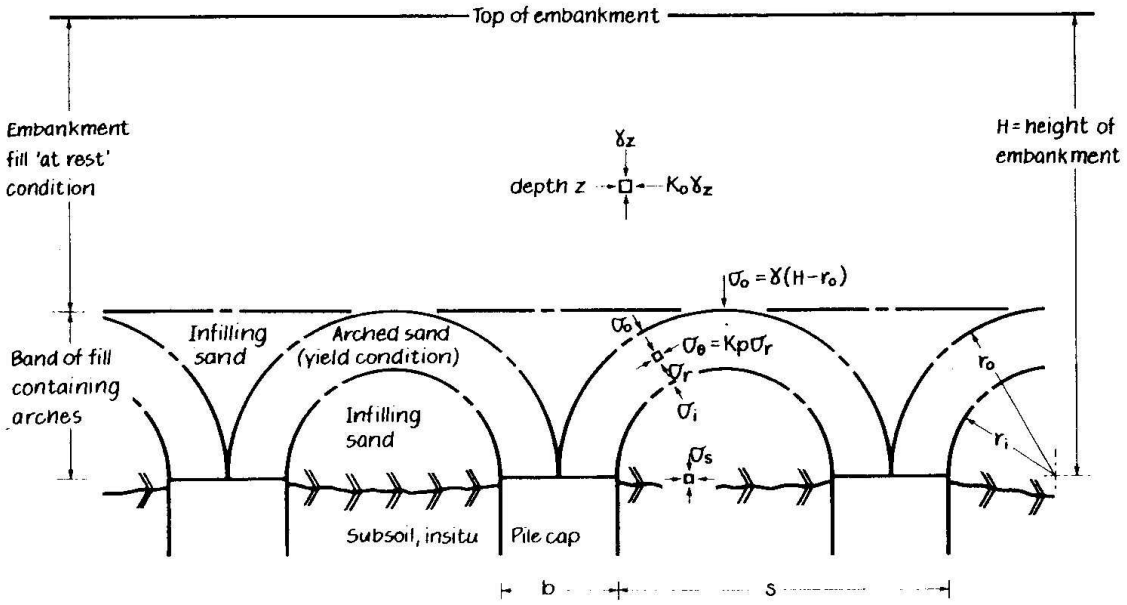

Figure 2.5: Section through a piled embankment showing the sand arches (from Hewlett & Randolph, 1988)

In Hewlett & Randolph`s formulation two different cases were considered. The first one is the plain strain geometry case, where the model tests showed that the critical zone is located at the crown of the arch. Hewlett and Randolph (1998) observed that due to static equilibrium, these arches are semicircular, of constant thickness and do not overlap. The second case is that of a three dimensional grid of piles. Both cases will be reviewed in this section, starting with the plain strain geometry case.

Plain strain geometry

An element of arched sand at the crown of the dome is shown on Figure 2.6. If we consider the radial equilibrium of forces acting on this element we obtain the following differential expression:

$$\frac{d\sigma_R}{dR} + \frac{2(\sigma_R - \sigma_\theta)}{R} = -\gamma \tag{2.6}$$

Where γ represents the self weight of the overlying fill, $\sigma_R$is the radial stress and σ_θ is the tangential stress, which is related to the radial stress by the Rankine passive earth pressure K_p in the following way:

$$\sigma_\theta = \frac{(1+sin\varphi)}{(1-sin\varphi)}\sigma_R = K_p\sigma_R \tag{2.7}$$

Figure 2.7 shows a diagonal section of a pile cap and dome crown in an embankment of height H, with pile caps of width b and centreline spacing s. The boundary condition on the outside of the arch is simply given by the weight of the fill above the crown. The boundary condition in the interior of the arch considers the minimum possible radius of the soil arch, which is determined by the spacing of the piles.

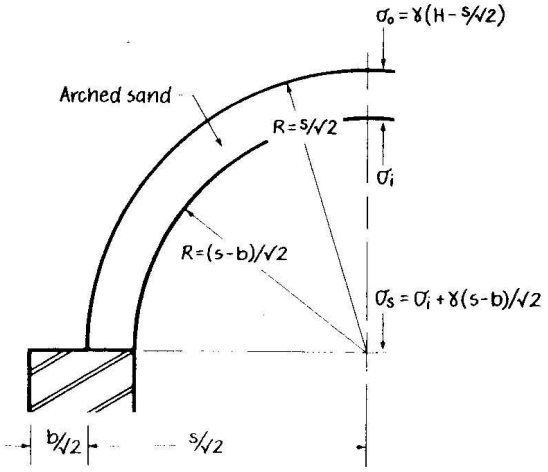

Figure 2.6: Arched sand at the crown of the dome, from Hewlett & Randolph (1988)

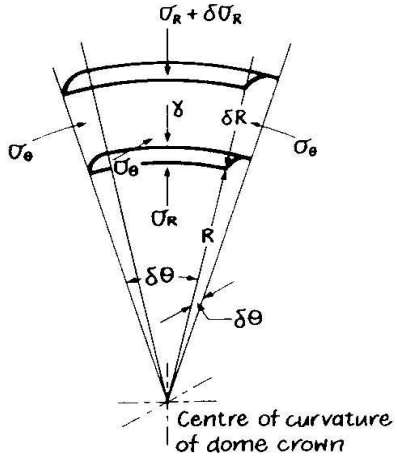

Figure 2.7: Sketch of the crown of a sand arch, from Hewlett & Randolph (1988)

Therefore the two boundary conditions described previously are:

at R = s/$\sqrt{2}$ $\sigma_o = \gamma(H - s/\sqrt{2})$ (2.8)

at R = (s-b)/ $\sqrt{2}$ $\sigma_R = \sigma_i$ (2.9)

Solving equation 2.7 subject to these boundary conditions leads to the following expression for the stress in the interior of the arch σ_i:

$$\sigma_i = \gamma \left(H - \frac{s}{2}\right) \left(\frac{s-b}{s}\right)^{(K_p - 1)} \quad (2.10)$$

The stress at the level of the geosynthetic σ_s is given by the sum of the stress σ_i and the weight of the fill between the arch and the geosynthetic, which leads to the following expression:

$$\sigma_s = \sigma_i + \gamma(s - b)\sqrt{2} \quad (2.11)$$

Grid of Piles

Models tests for the case of a three dimensional grid of piles suggest the formation of a series of domes forming a vault spanning between the pile caps, as shown on Figure 2.9. In this case, due to the limited area of support at the pile caps, the failure may also occur at the pile caps. Therefore the region of the crown arch and the region pile cap can fail independently and have to be analysed separately.

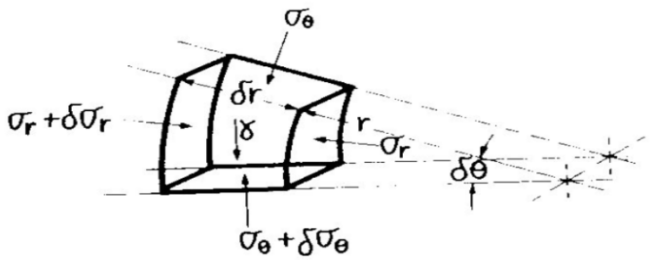

Figure 2.8: Arched element of sand at the pile cap (from Hewlett & Randolph, 1988)

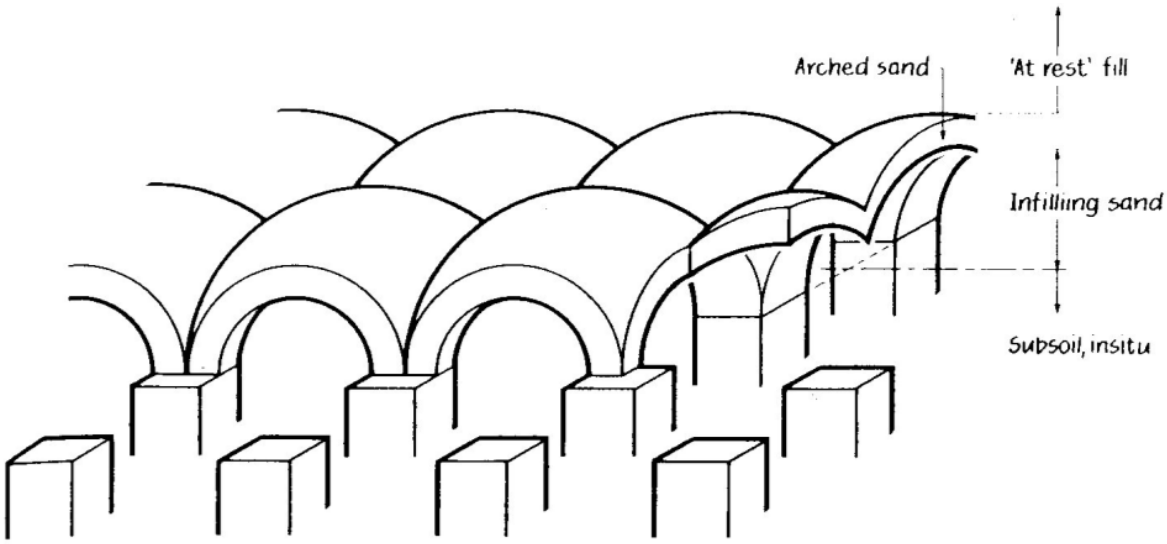

Figure 2.8: Domes forming a vault spanning between the grid of pile caps (from Hewlett & Randolph, 1988)

a) Crown of arch

Taking into account the spherical geometry and the inclusion of self weight, and proceeding in a similar way as in the plain strain case, the following expression for the total stress at the level of the geosynthetic may be found:

$$\sigma_s = \frac{\gamma(s-b)}{\sqrt{2}}\left(\frac{2K_p-2}{2K_p-3}\right) + \gamma\left(\frac{s-b}{s}\right)^{2K_p-2}\left\{H - \frac{s}{\sqrt{2}}\left(\frac{2K_p-2}{2K_p-3}\right)\right\} \quad (2.12)$$

b) Pile cap

In this case we have to consider the strongest of the 4 plain strain arches which constitute the vault, each of them occupying a quadrant of the pile cap. The strongest arch is the one which transfers the most load to the pile cap, and therefore it is the arch with the shortest span. By considering the radial equilibrium on an element of arched sand, as shown on Figure 2.9, the following equation is obtained:

$$\sigma_\theta = \sigma_r + r\frac{\partial \sigma_r}{\partial r} \quad (2.13)$$

The necessary boundary condition is given by the radial stress at the edge of the pile cap. Given that that the level of the cap the radial stress is horizontal, it will be equal to the pressure σ_s due to the weight of the fill. Hence the boundary condition is given by:

At $r_{inner} = (s-b)/2$ $\sigma_{rinner} = K_p p$ (2.14)

Solving equation 2.13 subject to this boundary condition we can obtain an expression for the radial stress:

$$\sigma_r = K_p p\left(\frac{s-b}{2r}\right)^{(1-K_p)} \quad (2.15)$$

If we integrate the tangential stress of the four arches which span onto each cap acting across

the area of the cap, assuming it is equal to$K_p\sigma_r$, the total force that can be supported by the file cap may be found. The condition of overall equilibrium imposes the following equation:

$$s^2\gamma H = F + p(s^2 - b^2) \tag{2.16}$$

Hence the total force is:

$$\mathrm{F} = \frac{\gamma H}{\left(\left(\frac{2K_p}{K_p+1}\right)\left\{\left(\frac{s-b}{2r}\right)^{(1-K_p)} - \left(1-\frac{b}{s}\right)\left(1+K_p\frac{b}{s}\right)\right\} + \left\{1-\frac{b^2}{s^2}\right\}\right)} \tag{2.17}$$

Limitations of the model

Hewlett & Randolph's formulation, as well as Terzaghi's, is based on a fill material which is drained, homogeneous and isotropic, and it assumes that the soil does not dilate during shearing, which in practice would reduce the surface settlements.

Potts (2007) noted that the major limitation for the implementation of Hewlett & Randolph's formulation for the case of a void forming under a geosynthetic reinforced fill is that this formulation is derived for the case of a grid of piles. The soil arches which are assumed to form between the pile caps have a maximum thickness controlled by the thickness of the pile caps, b/2. This determines one of the boundary conditions used to determine the maximum stresses acting at the level of the geosynthetic. In our case of study there is no such physical constraint to the extent of these arches, and therefore the boundary conditions and the final solutions should be modified.

2.4 Comparison of Arching theories

Potts (2007) compared the results of a finite element analysis of a void of vertical sides forming under a geosynthetic reinforced layer with Hewlett & Randolph's formulation and Terzaghi's arching theory. The vertical stress profile above the void proposed by both theories was compared with the results of the finite element analysis with the aim of determining which if the two is most appropriate. In the following sections the vertical stress profiles according to both theories, as well as the results and conclusions obtained by Potts (2007) will be described.

2.4.1 Vertical stress profile according to Terzaghi's Arching theory

The vertical stress profile in Terzaghi's formulation is a function of the height z above the void, the fill properties and the stress ratio K, and is given by:

$$\sigma_v = \frac{D(\gamma - \frac{2C}{D})}{2K\tan\varphi}\left(1 - e^{\frac{-2Kz}{D}\tan\varphi}\right) + w_s e^{\frac{-2Kz}{D}\tan\varphi} \tag{2.18}$$

The vertical stresses corresponding to this equation are sketched on Figure 2.10 (dotted line), in the case that there is no surface charge load.

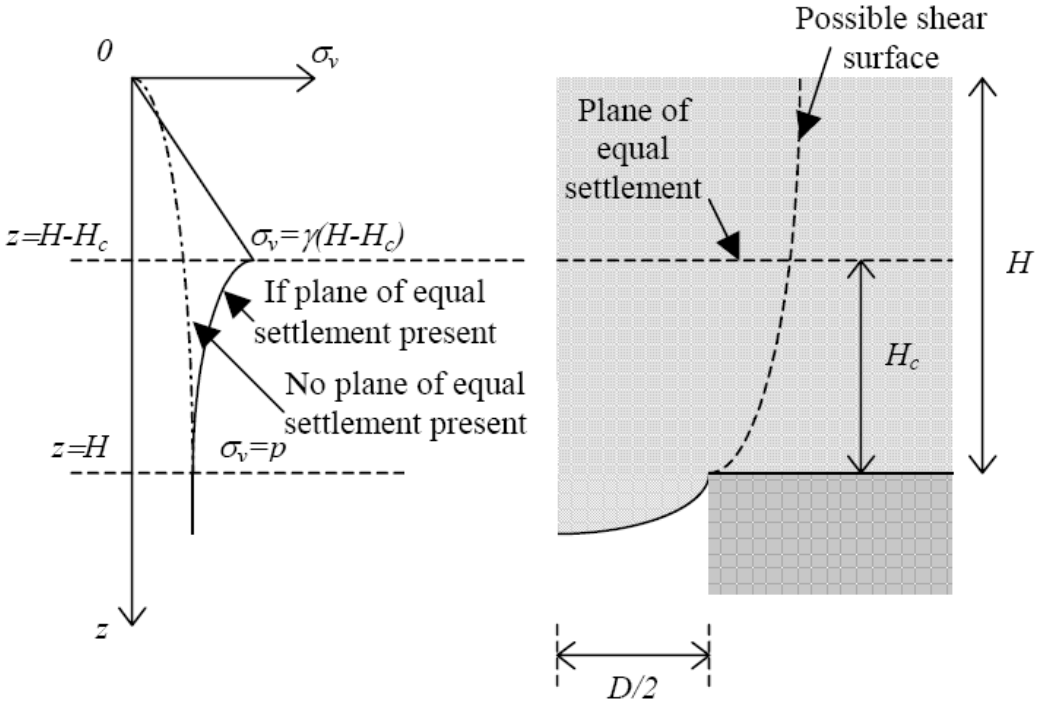

Figure 2.10: Vertical stress distribution according to Terzaghi's arching theory (from Potts, 2007)

However equation 2.18 is only valid when the area where the vertical stresses are affected by the presence of the void propagates up to the surface of the fill. If the fill is sufficiently deep a plane of equal settlement may be identified above which the fill remains undisturbed. Hence in these cases equation 2.18 is no longer valid, and the stress profile is the one represented by the solid line. The vertical stress increases linearly until the plane of equal settlement which lies at height H_c, and then it tends asymptotically to the stress profile predicted using equation 2.18.

Therefore, the identification of the critical height H_c at which the plane of equal settlement forms becomes crucial in order of predicting the vertical stress profile. Terzaghi suggests that this height is approximately equal the width of the void D, based on experimental observations.

2.4.2 Vertical stress profile according to Hewlett & Randolph

A sketch of this profile for the case in which there is no surcharge load on the surface and assuming that the soil arch has a thickness b is shown in Figure 2.11.

In this formulation it is assumed that the fill remains undisturbed above the crown of the arch and therefore the vertical stress profile corresponds to the hydrostatic stress profile, increasing linearly with a slope governed by its self weight. Within the arch the stress then decrease linearly until they reach a certain value σ_i at a height corresponding to the inner radius of the soil arch. This inner radius corresponds to the half of the void width, D/2. Underneath the soil arch the stresses then increase linearly again, reaching a stress at the level of the geosynthetic given by

$$F = \frac{\gamma H}{\left(\left(\frac{2K_p}{K_p+1}\right)\left\{\left(\frac{s-b}{2r}\right)^{(1-K_p)} - \left(1-\frac{b}{s}\right)\left(1+K_p\frac{b}{s}\right)\right\} + \left\{1-\frac{b^2}{s^2}\right\}\right)} \quad (2.19)$$

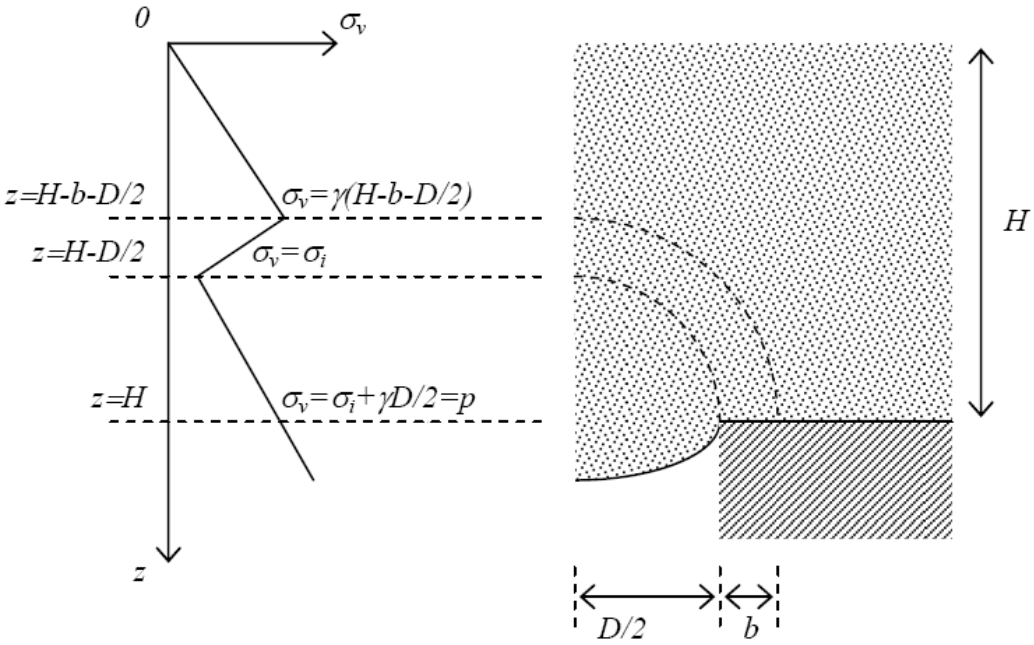

Figure 2.11: Vertical stress distribution according to Hewlett & Randolph's formulation (from Potts, 2007)

The major problem with this formulation is that there is no theoretical value for of the width of the soil arch (b) in the case of a void forming beneath a geosynthetic reinforce layer. Potts proposed that this value could be estimated by identifying the height at which the maximum vertical stresses occur. Since the inner radius of the soil arch does have a physical restraint and is equal to D/2, the value of b would be the height at which the peak stress occurs minus D/2.

2.4.3 Comparison of arching theories for a vertical sides void by Potts (2007)

As mentioned in previous sections, Potts (2007) analysed the soil arching effect in a geosynthetic reinforced fill above a vertical sides void by means of finite element analysis. A sketch of the typical mesh used in this analysis is shown on Figure 2.12, in which only half of the problem was modelled due to the horizontal symmetry.

The model was created using the Imperial College Finite Element Program (ICFEP), and generally only one layer of geosynthetic was modelled. The formation of circular and longitudinal voids underneath the geosynthetic layer were analysed by conducting axisymmetric and plane strain analyses respectively. The properties of the fill material, the foundation soil and the geosynthetic used for most of these analyses are the ones summarised in table 2.1.

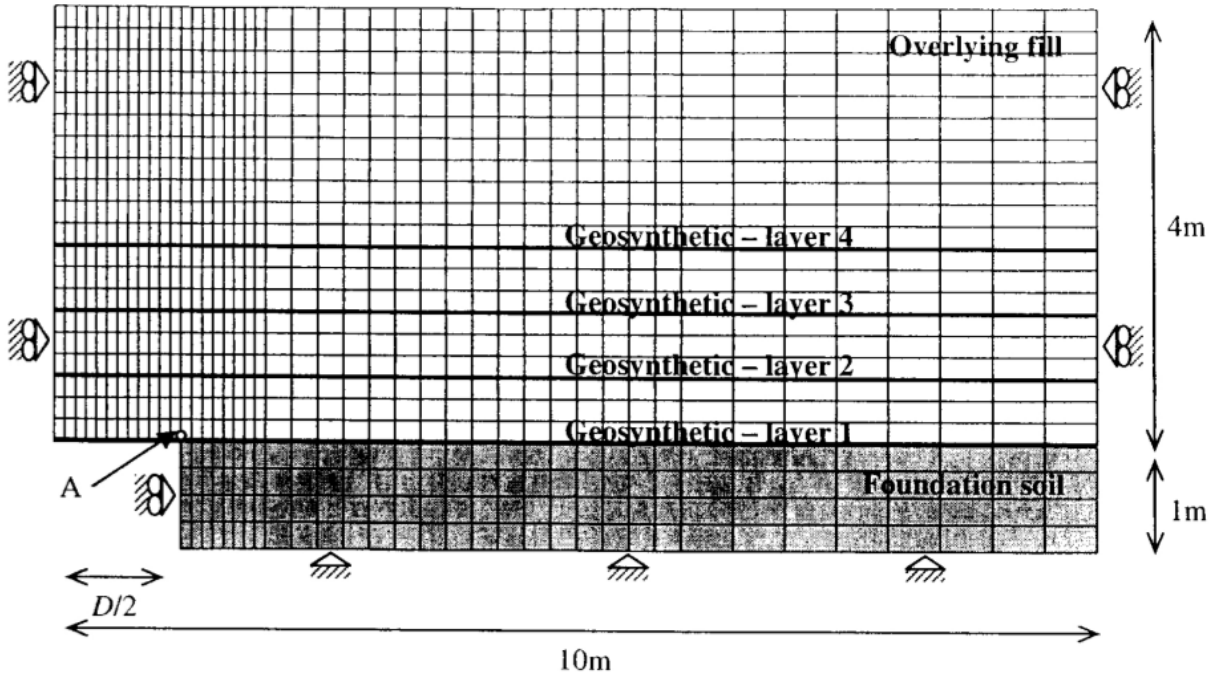

Figure 2.12: Finite element mesh used for the parametric study by Potts (2007)

Material	Parameters
Fill	K_o = 0.43; γ = 20kN/m^3; E = 20,000kN/m^3 μ_f = 0.3; c' = 0kPa φ' = 35 º; ν = 0 º
Foundation soil	J = 50kN/m; t=5mm; μ = 0.2; T_{ult} = 100kN/m
Geosynthetic	K_o = 0.43; γ = 20kN/m^3; E = 100,000kN/m^3 μ_f = 0.3; c' = 0kPa φ' = 35 º; ν = 0 º

Table 2.1: Material parameters

In these analyses the possible existence of a soil arch could be identified by considering the stress distribution in the fill layer as well as the orientation of the major principal stresses. The plots of the orientation of the major principal stresses can be obtained from ICFEP, and two of these cases are shown in figures 2.13 and 2.14. Each line represents the direction of the orientation of the major principal stress in each element. If no void was present all of the lines would remain completely vertical.

Potts (2007) distinguished two different cases with respect to the orientation of the major principal stresses. In the first case, shown in Figure 2.13, the stresses remain unaffected by the presence of the void except in a confined region close to the void, whilst in the second case, which is shown in Figure 2.14, the disturbed fill propagates to the surface. The second case corresponds to bigger voids compared to the fill height, whilst the first one was typical of smaller voids. Both figures represent the case of an infinitely long void, analysed with plain strain geometry.

Potts (2007) noted that Hewlett & Randolph's formulation seemed appropriate when an arch of the form shown in Figure 2.13 could be seen, but it was not consistent with the mode of arching seen in Figure 2.14. On the other hand, Terzaghi's theory could be used to described

both cases depending on whether a plane of equal settlement was formed, as in Figure 2.13, or not, as in Figure 2.14. Therefore Terzaghi's theory is more generally applicable and the question remained on which of the two theories is more appropriate when the mode of arching seen in Figure 2.13 can be seen.

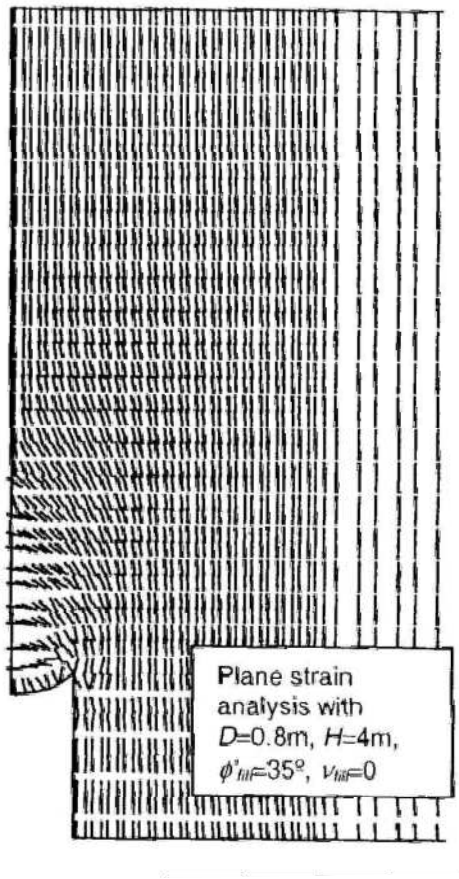

Figure 2.13: soil arch above which the soil is undisturbed (from Potts, 2007)

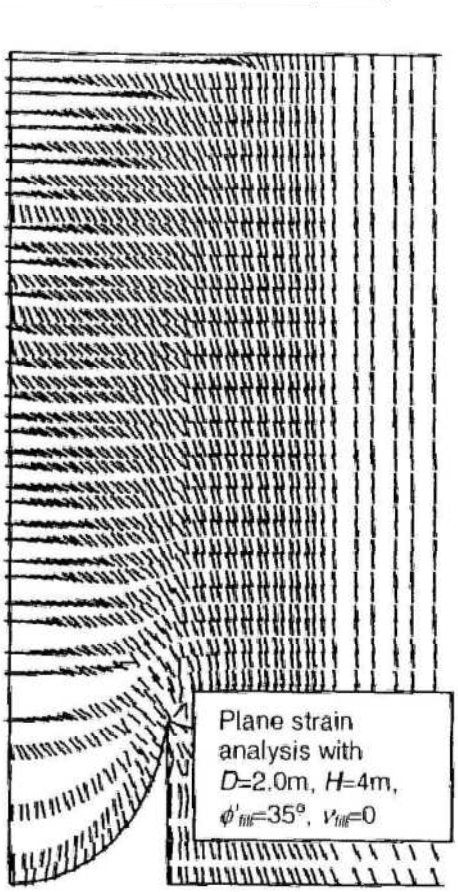

Figure 2.14: disturbed fill propagated to the surface (from Potts, 2007)

Mifsud (2005) performed a numerical analysis using a finite element model with ICFEP with the aim of further understanding the behaviour of geosynthetic reinforced fills when a vertical sides void forms beneath the geosynthetic, in a similar way as Potts (2007). Mifsud (2005) noted the importance in terms of surface settlements and tensile forces in the geosynthetic of the extent of the zone of the fill which is disturbed by the fill. Hence it is important to distinguish between the cases seen in Figures 2.13 and 2.14.

It was proposed that the disturbed zone in the fill, which is characterised by the rotation of the principal stresses, could be visualized as being contained in an imaginary 'bubble', which rises from the void, having larger deformations and surface settlements as more of the top part of the bubble reached the surface of the fill (Figure 2.15). Mifsud also analysed the effects of the compaction properties of the overlying fill layer, and the results of this work will be discussed further in this chapter.

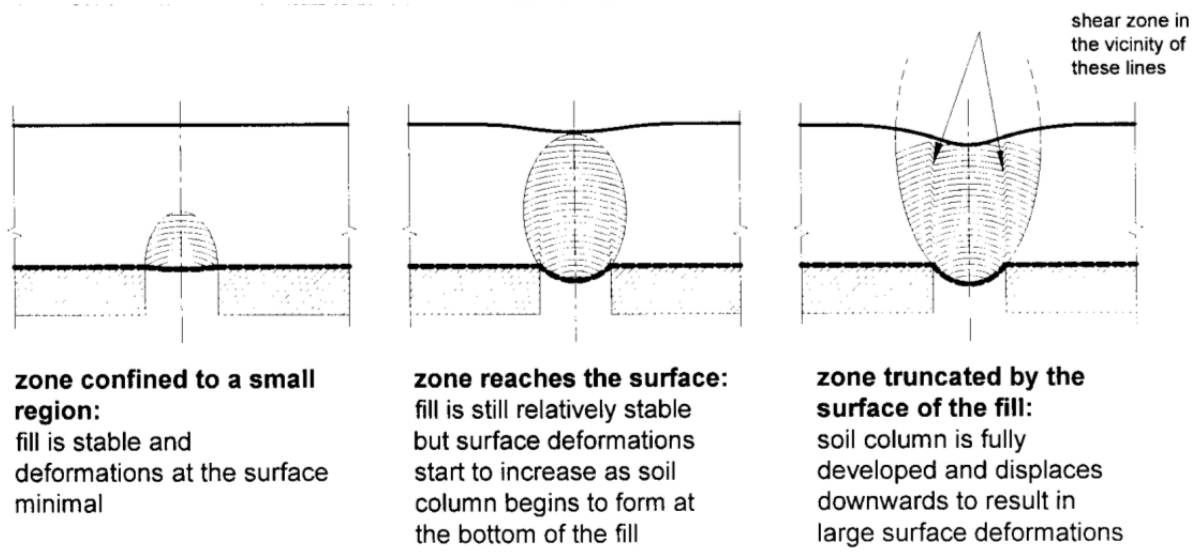

Figure 2.15: Representation of the extent of fill which is disturbed by the presence of the void (from Mifsud, 2005)

The question of which of the two theories is more appropriate when the mode of arching seen in Figure 2.13 can be seen was initially addressed by comparing the vertical stress profiles in the fill above the centreline of the void obtained analytically with those predicted by both theories. Figures 2.16 and 2.17 show the stress profiles in the fill above circular and longitudinal voids for different widths. With all of the widths considered in these plots the disturbed fill was not propagated to the surface and the height of the overlying fill was 4m. Hence these are the stress plots for which it was still not clear which if the two arching theories was more appropriate.

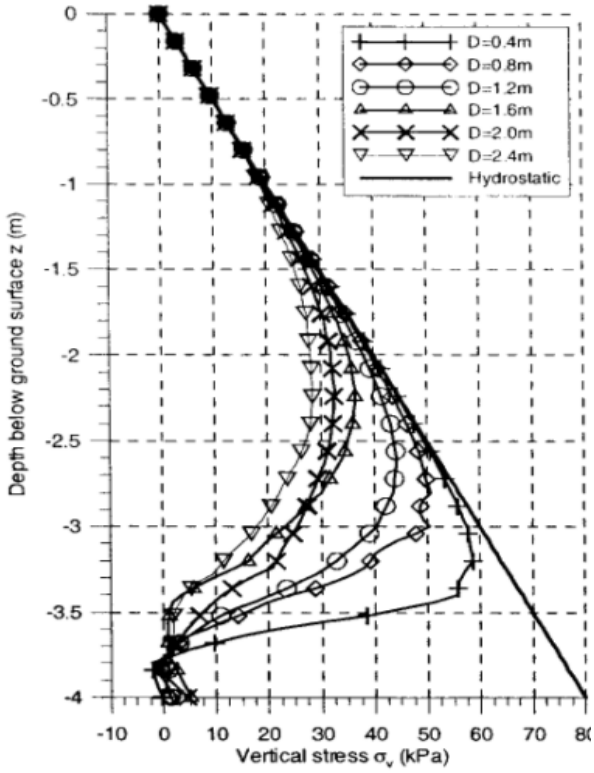

Figure 2.16: Vertical stress profiles above the centre of circular voids of different widths (from Potts, 2007)

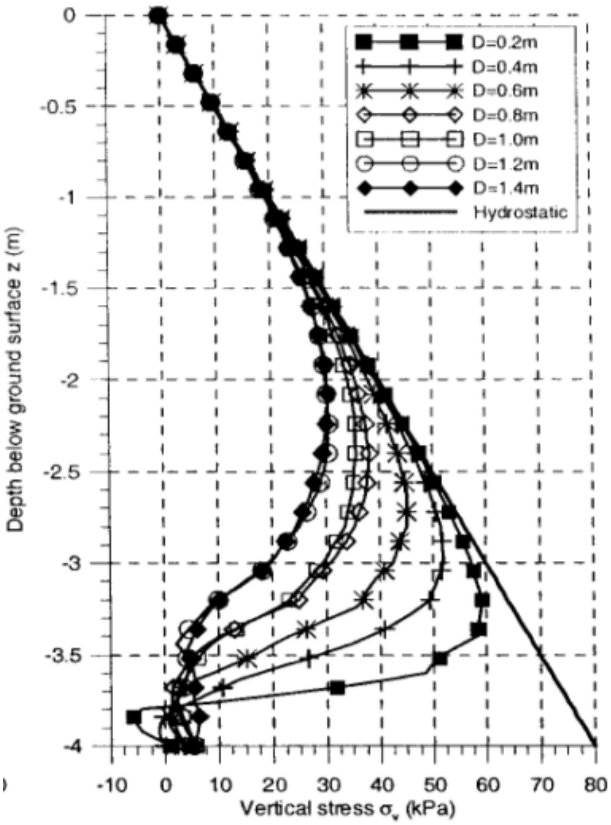

Figure 2.17: Vertical stress profiles above the centre of circular voids of different widths (from Potts, 2007)

The main difference between Terzaghi's theory and Hewlett & Randolph's approach regarding the vertical stress profiles in the overlying fill is what happens to the stresses beneath an arch. In Terzaghi's approach the stresses tend asymptotically to a constant value, whilst with Hewlett & Randolph's approach the vertical stresses continue to increase at the same rate as before reaching the soil arch.

This question of which of the two theories is more appropriate was further clarified by Potts (2007) by considering contours of stress level in the fill. These are a measure of the ratio of the current shear stress in the fill to the available shear stress, and are therefore useful for identifying the zones in the fill that are subjected to high stress levels. If an arch as the type proposed in Hewlett & Randolph's formulation should form then the major principal stresses should be tangential to this arch.

Potts (2007) noted that this phenomenon could not be detected by considering the vertical or horizontal stresses alone, and hence used the contours of stress level. Figures 2.18 and 2.19 show the stress contours above a 2.6m circular void and a 1.4m infinitely long void respectively, which correspond to the maximum void widths at which the mode or arching shown in figure 2.13 could still be seen. The orientation of the major principal stresses in the fill are also plotted in these figures.

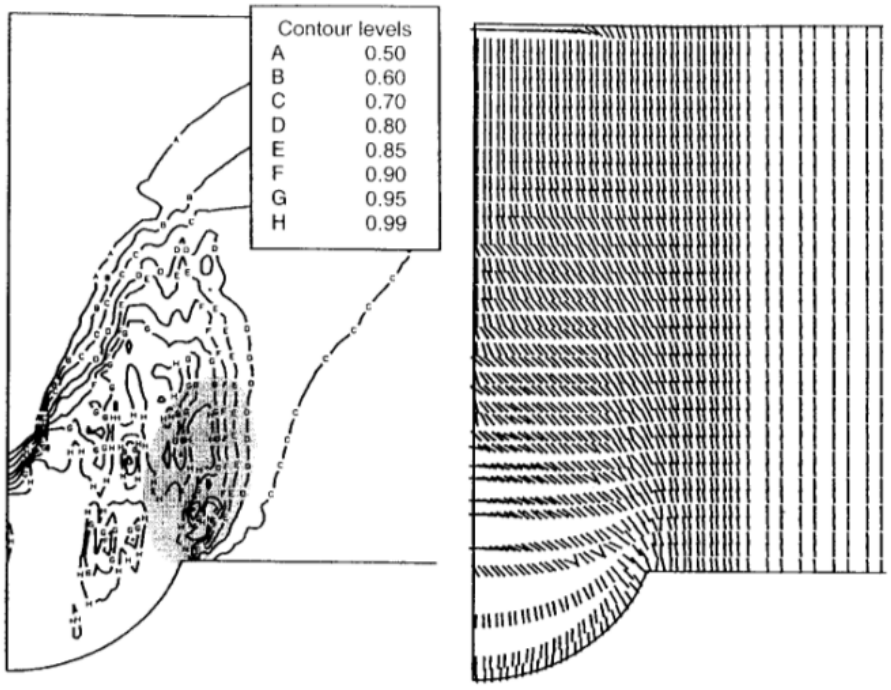

Figure 2.18: Stress regime in the fill above a 2.6m circular void (from Potts, 2007)

Figures 2.18 and 2.19 prove that the maximum stress levels occur at the corners of the void, and then propagate vertically upwards. Hence they do not follow the shape of an arch that we would expect from Hewlett & Randolph's formulation, and it is only consistent with Terzaghi's theory.

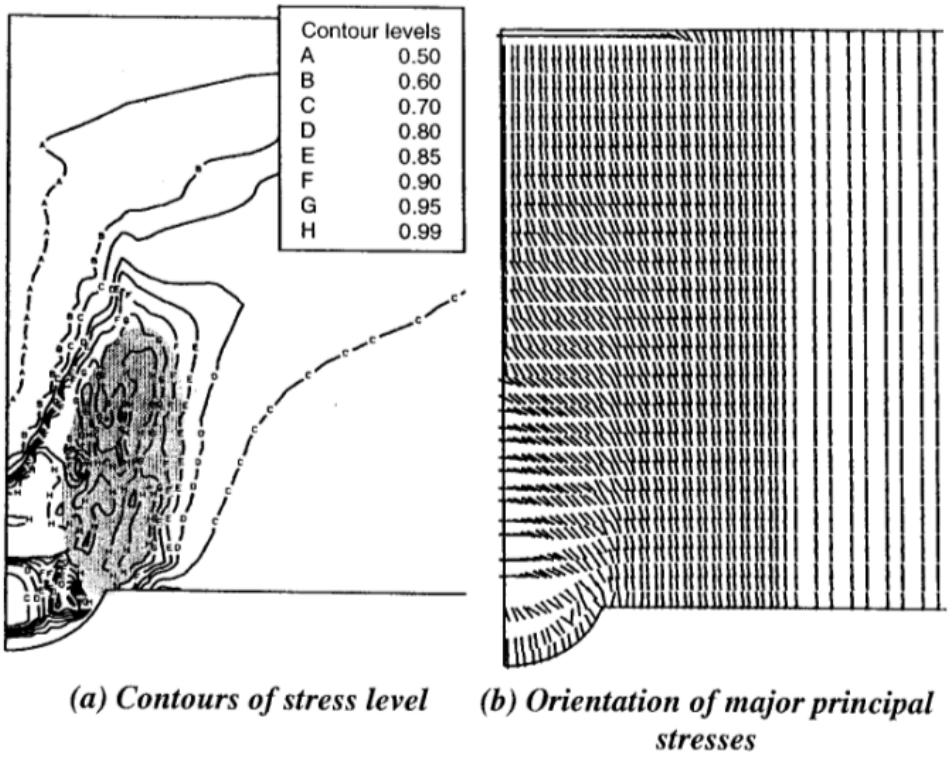

Figure 2.19: Stress regime in the fill above a 1.4m infinitely long void (from Potts, 2007)

The conclusion that Hewlett & Randolph's approach may not be appropriate was further corroborated by considering the orientation of the principal stresses in the cases when there was a depth of fill unaffected by the void. In these cases it was seen that the orientation of the major principal stresses were not tangential to the curve if the arcs proposed in Hewlett & Randolph's theory. This can be seen in figure 2.20. Hence, for the case of vertical sides void forming under geosynthetic reinforced layer Potts (2007) concluded that Terzaghi's theory is more appropriate. One of the aims of this paper is to determine whether the alteration of the shape of the voids will alter this conclusion.

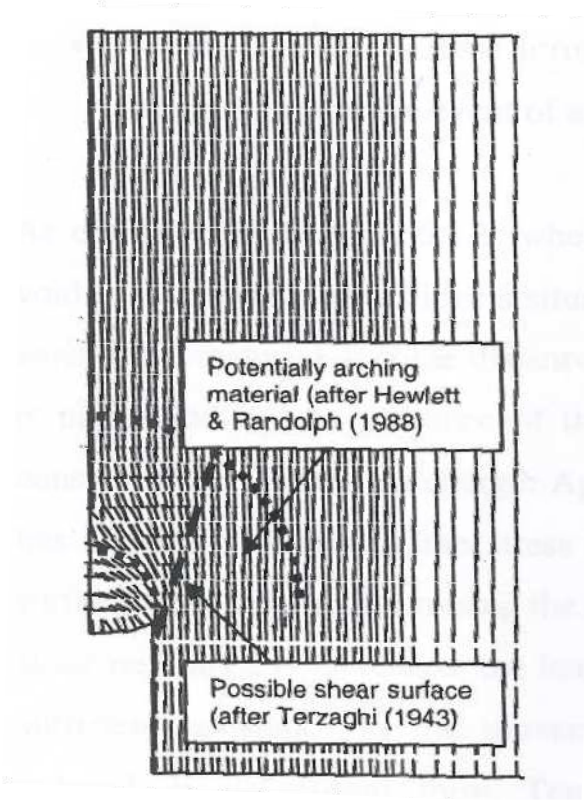

Figure 2.20: Orientation of the major principal stresses above a 0.8m wide circular void (from Potts, 2007)

2.5 Behaviour of the Geosynthetic

In the numerical analysis done by Potts (2007) the behaviour of the geosynthetic in terms of the shape of the deformed geosynthetic and the strains and stresses developed was analysed, again for the case of a vertical sides void, as shown in Figure 2.12.

Two different shapes of the deformed geosynthetic are proposed by the available design methods: a circular arc or a parabolic arc. These two shapes are the result of two different approaches to the stresses developed in the fill. A parabolic shape is a consequence of assuming that the stresses acting at the level of the reinforcement are purely vertical at all the locations across the void width. On the other hand, to assume that the deformed shape of the geosynthetic can be approximated by a circular arch implies that the stresses acting on the geosynthetic are at all locations normal to the geosynthetic. Hence this latter approximation assumes that the stresses at the level of the geosynthetic have also a horizontal component, except in the centre of the void.

Potts (2007) noted that some load transfer mechanism always developed in the fill, even if a stable arch was not formed. This transfer mechanism is due to the interaction of the fill particles when they move relative to each other. This means that there is also some horizontal component in the stress at the level of the geosynthetic, therefore invalidating the assumption of a parabolic arc for the shape of the deflected geosynthetic. Hence theoretically, the circular arc approximation seems more appropriate.

This was corroborated with a finite element analysis by Mifsud (2005), in which the shape of the deflected geosynthetic was compared with the circular and the parabolic arc. Figure 2.21 shows a representative example of his findings.

Both the parabolic and the circular arc slightly underestimate the geosynthetic deflection, although it is clear that as expected, the circular arc provides a better approximation than the parabolic arc, for the case of a vertical sides void. A question which aims to be clarified in this study is whether the circular arc will still be the best approximation for the shape of the deflected geosynthetic when the void which forms beneath the geosynthetic has its sides with a certain inclination respect to the horizontal.

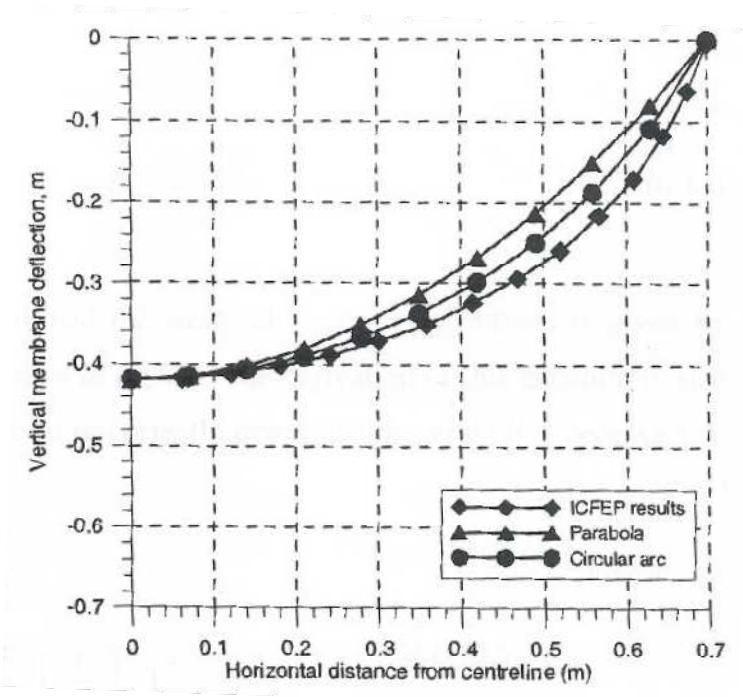

Figure 2.21: Shape of the deflected geosynthetic above a 1.4m longitudinal void (from Mifsud, 2005)

2.6 Effect of the Angle of Shearing Resistance

The effect of the angle of shearing resistance of the overlying fill, φ'_{fill}, for the case of a geosynthetic reinforced load transfer platform above a void of vertical sides was analysed in the work done by Potts (2007). It was seen that the deflections and the stresses developed in the geosynthetic were reduced as φ'_{fill} was increased for all of the void widths considered and for both circular and longitudinal voids.

The reduction of stresses at the level of the geosynthetic indicates that there is a load transfer mechanism acting on the fill. Therefore, higher values of φ'_{fill} enables to bridge wider voids

since a stable arch is more easily formed. The possible transfer mechanisms can be identified by considering the plots of the orientation of the major principal stresses in the fill. Figure 2.22 shows these plots in a fill layer above a 1.4m wide longitudinal void with two different values of φ'_{fill}.

The formation of a soil arch can only be identified for the case where $\varphi'_{fill} = 45^0$, where there is some part of the fill which is undisturbed by the presence of the void. In the case where $\varphi'_{fill} = 25^0$ the disturbed fill propagates up to the surface.

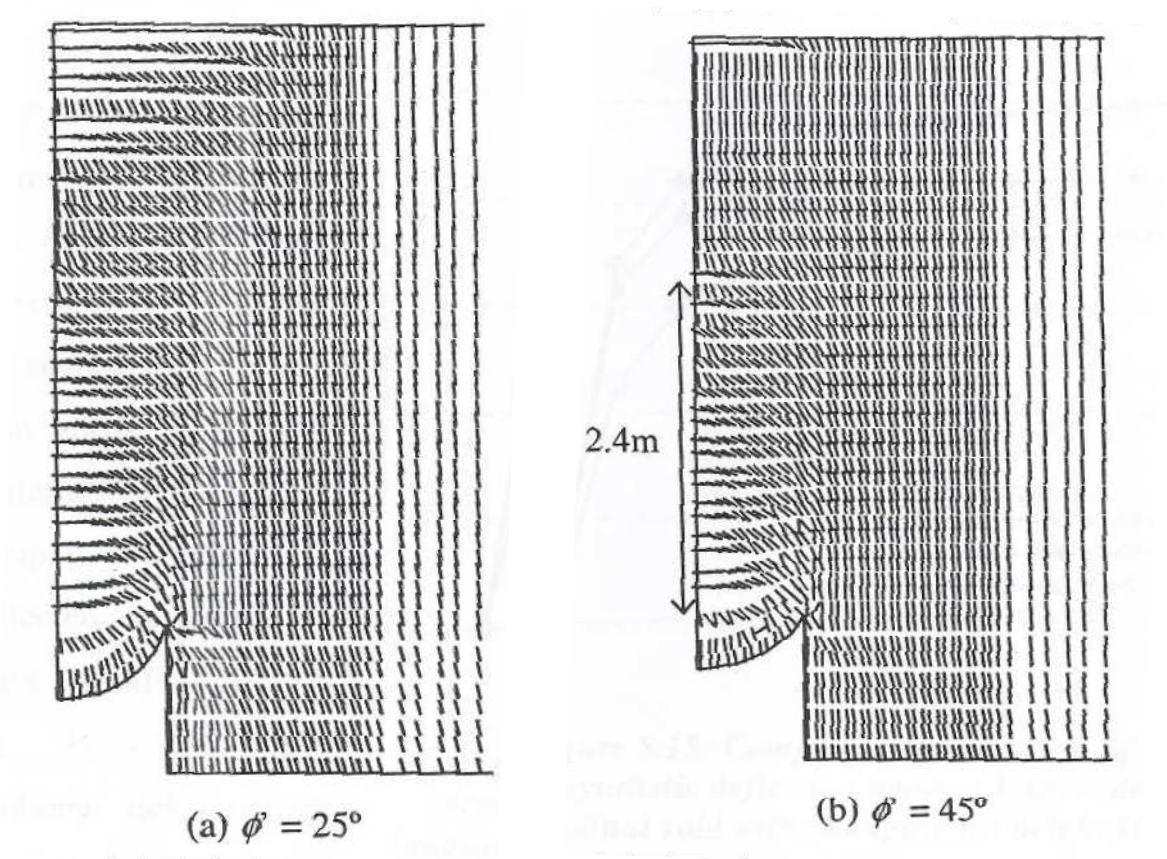

Figure 2.22: Orientation of the major principal stresses above a 1.4m wide longitudinal void of two different values of the angle of shearing resistance of the fill, (from Potts, 2007)

2.7 Soil suction

The level of soil suction in the fill is the most important compaction property and it depends strongly on the water content of the fill. Soil suction only occurs in an unsaturated soil and can be found in all ground above the water table. It represents the state of the soils ability to attract water and it can be seen as a negative pore pressure. The meniscus which forms between particles produces a normal force between the adjacent particles resulting in a temporary bond which tends to increase the strength of the soil. Therefore the soil suction should have a positive effect on the stability of the overlying fill in the geosynthetic reinforced load transfer platform studied in this project.

The magnitude of the attraction that the soil exerts on the water depends on many factors such as its structure and bulk density, on the moisture of the soil and on the temperature (Arvind, 2003). The most important of these factors is the moisture content of the fill. The moisture content of the fill is a typical compaction parameter which can be controlled during the

construction of the fill embankment.

The numerical analysis performed by Mifsud (2005) presented in section 2.4.3 also considered the influence of the compaction properties on the behaviour of a geosynthetic reinforced fill overlying a void. In particular the effects of soil suction within the overlying fill were analysed, considering 3 possible values of suction: 5kPa, 10kPa and 20kPa.

It was seen that different values of suction resulted in very different geosynthetic deformation and stresses, ranging from almost zero when the soil suction is high to considerably large deformations and stresses with lower values of suction. Similarly, surface settlements also increased with lower values of the soil suction within the fill. This can be seen in Figures 2.23 and 2.24. As expected, higher values of the geosynthetic tensile stress were obtained with lower values of the soil suction. In these figures, PS represents the plain strain geometry case, i.e. the case of an infinitely long void and AS represents the axisymmetric case, i.e. the case of a circular void.

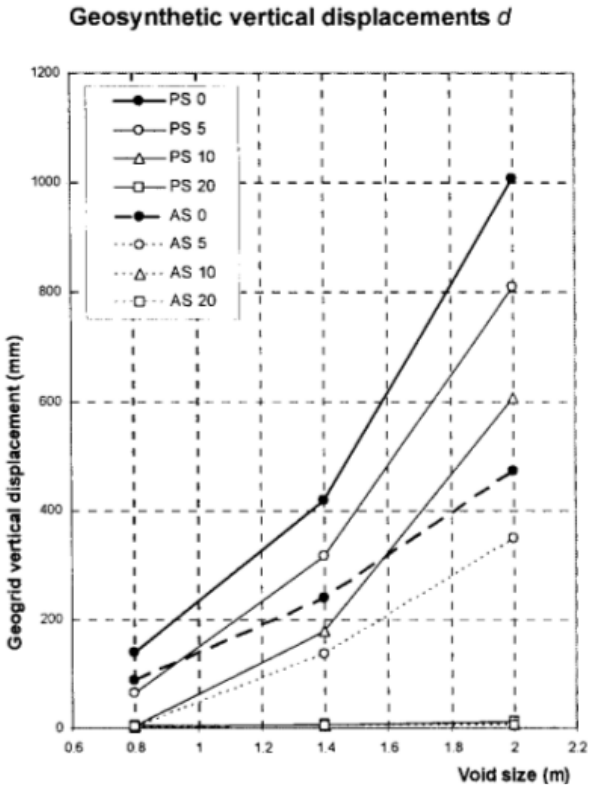

Figure 2.23: Variation of the geosynthetic vertical displacement with the soil suction (from Mifsud, 2005)

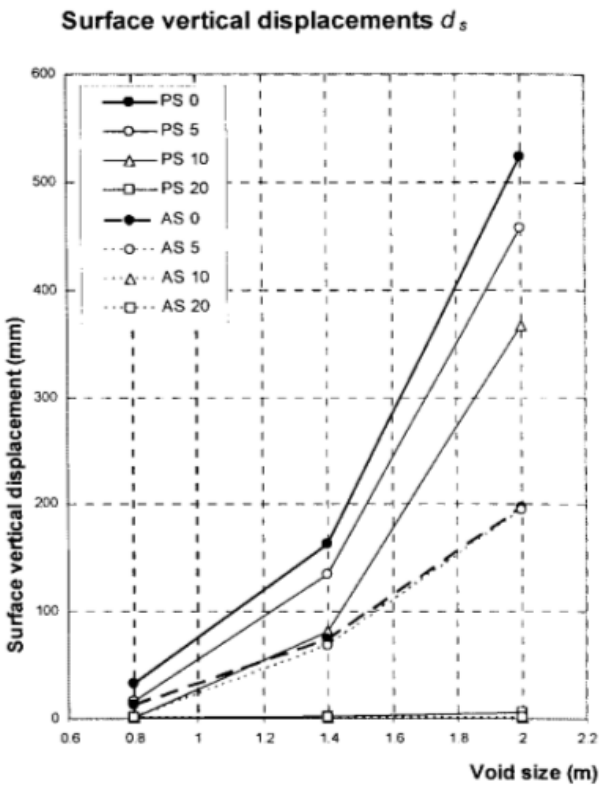

Figure 2.24: Variation of the surface vertical displacement with the soil suction (from Mifsud, 2005)

Mifsud (2005) noted that the smaller deformations which occur with higher values of soil suction can be explained by considering the failure criterion adopted, which as well as in the case of study of this project, was the Mohr Coulomb failure criterion. Higher soil suction values are essentially greater negative pore pressures, which result in a higher effective stress. According to this failure criterion higher shear stresses can be supported with higher values of the effective stress.

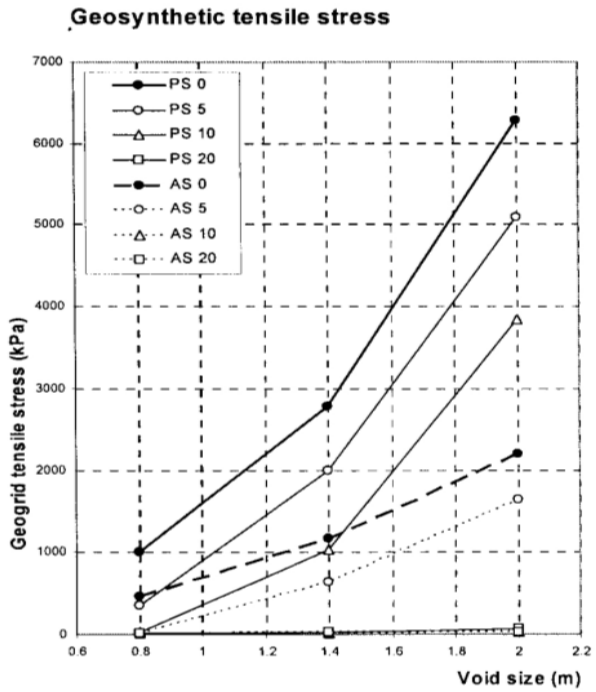

Figure 2.25: Variation of the geosynthetic tensile stress with the soil suction (from Mifsud, 2005)

An example of how the deformations and stresses can vary considerably if the water content in the fill changes was analysed by simulating a flooding process. Flooding was identified by Terzaghi (1943) as a factor which can cause a stable arch to breakdown. The flooding process was modelled using ICFEP for the case of a 4m high fill and with varying void widths, shapes and angles of dilation.

Figure 2.26 and 2.27 shows how the surface settlements and the vertical geosynthetic displacements increase considerably with flooding. Mifsud (2005) concluded that the reduction in the effective stress caused by flooding caused the area of disturbed fill to grow towards the surface, in a progressive manner. It was also concluded that soil arching can exist to different degrees, and therefore the notion of a single soil arch which can be completely destroyed by an external influence such as vibration or flooding is not correct.

Figure 2.25 shows the geosynthetic tensile stress for the different combinations of shape and level of soil suction in the overlying fill.

The results of this numerical analysis clearly highlight the positive effects of considering the level of soil suction in the overlying fill, although Misfud (2005) also noted the potential danger of assuming a constant value of the suction, since it can vary rapidly if the moisture content in the fill changes. If the soil suction decreased, the effective stresses would also decrease resulting in larger stresses and deformations in the geosynthetic. Hence the positive effects of modelling the soil suction in the fill have to be taken with precaution.

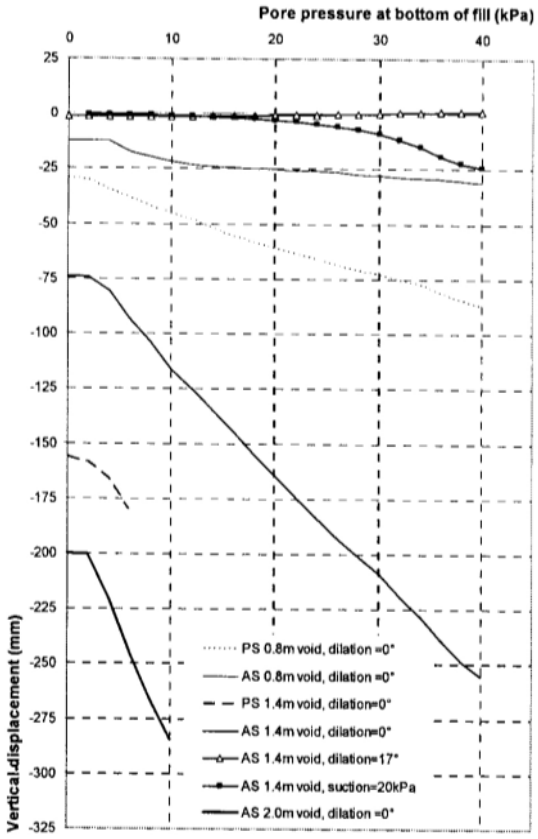

Figure 2.26: Variation of surface vertical displacements as flooding progresses (from Mifsud, 2005)

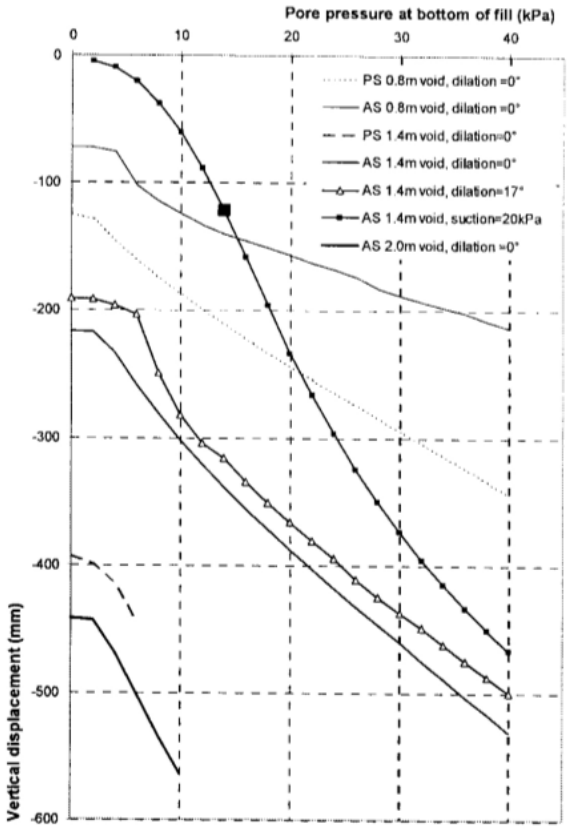

Figure 2.27: Variation of geosynthetic vertical displacements as flooding progresses (from Mifsud, 2005)

Chapter 3: Research Strategy

The main objective of this study is to investigate the effects of a void forming beneath a geosynthetic reinforced fill layer. This problem was already addressed by Pottts (2007) considering the formation of a void of vertical sides, as it was described in the previous chapter. What needs to be addressed in this study is the effects of varying the void's shape in the formation of a soil arch. In particular, the cases in which the side of the void has an inclination of 45º or 60º will be considered. A sketch of this design scenario can be seen in figure 3.1.

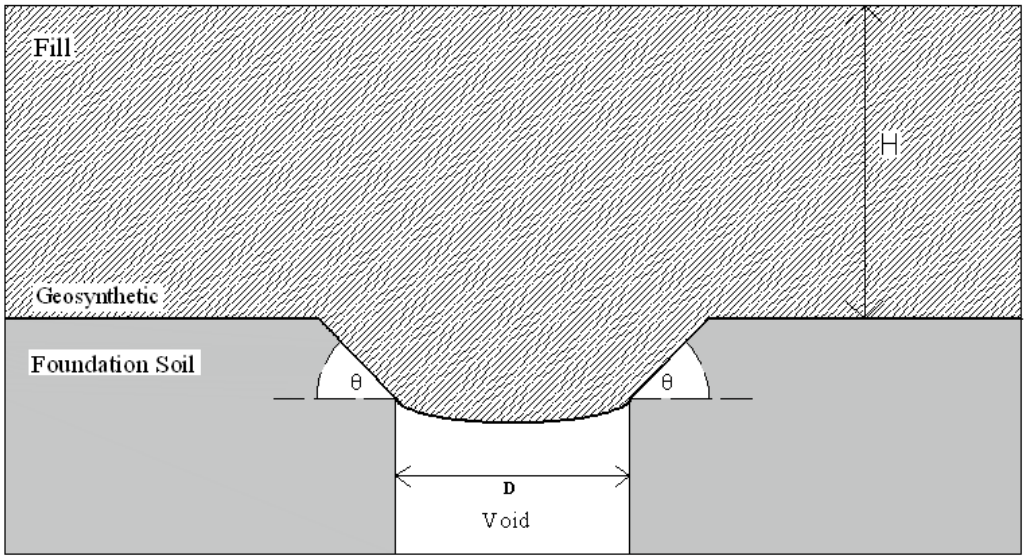

Figure 3.1: Sketch of the design scenario

The potential effects on the arching behaviour of varying the angle of shearing resistance of the fill can also be considered as one of the main aims of the study. Finally, the effect of soil suction in the fill material will also be analysed.

The objectives of this study can be achieved by means of a numerical analysis, in particular by considering a finite element method analysis. The potentially best method of analysis capable of solving engineering problems such as the one presented in this paper is a full numerical analysis. Within a numerical analysis, the finite element method will be used in this study, using the Imperial College Finite Element Program (Potts & Zravkovic, 1999).

The main reason for using the finite element method for this study is that it has been demonstrated (Potts, 2007) that this method produces realistic results for these types of problems. The validation of this method was achieved in two ways:

1) By comparing the results of a case study with those obtained using the finite element method using ICFEP. The case study chosen was the construction of three embankments built on soft Bangkok clay, in which the results predicted by ICFEP were seen to fit well with the real observed measurements. In particular this proved that the use of membrane elements to model the geosynthetic was appropriate.

2) In order of assessing the validity of this method when a void is formed beneath a reinforced soil layer a series of model tests were done. It was seen that the results of the finite element analyses produced fairly similar results to the model tests.

3.1 Finite Elements and Constitutive Models

In the finite element method the first step is to model the geometry of the problem by subdividing it into small regions called finite elements, which contain nodes on the boundaries or within the element. In this case the finite element analysis was done on ICFEP using membrane elements to model the geosynthetic, eight-noded quadrilateral elements for the fill material and six-noded zero-thickness interface elements to model the soil-geosynthetic interface in some cases. The primary variable adopted was the displacement. Due to the 2-D nature of the problem of this study, the independent variables for each node are the horizontal and vertical displacements, u and v. All of the elements used are isoparametric, i.e., they use the same shape functions to describe the geometry and the displacements.

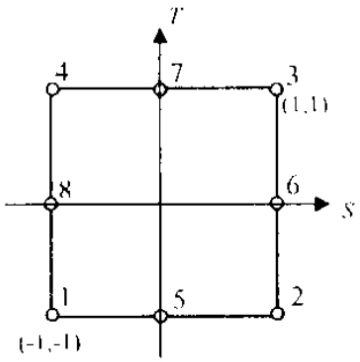

Figure 3.2: 8 noded isoparametric element (from Potts & Zdravkovic, 1999)

The three different materials which are analysed in this study are the fill material, the geosynthetic and the foundation soil, which were modelled in the same way as in the numerical analysis done by Potts (2007) in order to be able to compare the results obtained in this study. The way in which these materials were modelled on ICFEP is described in the following sections.

3.1.1 Solid elements

The fill material and the foundation soil were modelled as elastic-perfectly plastic materials with a Mohr-Coulomb failure criterion given by:

$$\tau = c' + \sigma_n \tan\varphi' \qquad (3.1)$$

The elasticity of the soil is governed by the Young´s modulus E and the Poisson`s ratio μ.

3.1.2 Membrane elements

The geosynthetic layer was modelled as membrane elements, which are useful to represent elements which cannot transmit bending moments or shear forces. It is similar to a spring, only differing in that it can be curved and it is treated as all the other elements in the analysis (Potts & Zdravkovic, 1999). The membrane elements used were the same as in the numerical analysis done by Potts (2007), i.e. three-noded isoparametric line elements, since the use of such elements was proved to be appropriate for this case. As well as the solid elements, they

were modelled as elastic-perfectly plastic materials, governed by the constant tensile stiffness J and the ultimate tensile force T_{ult}.

3.1.3 Large Displacement Analysis:

Mifsud (2005) noted the need for a large displacement analysis in order to correctly model the effect of the geosynthetic. In a large displacement analysis the mesh is updated after each increment to reflect the possible changes in geometry. This allows the geosynthetic to bend and hence it can resist vertical loads. If no changes in the geometry of the mesh were permitted, i.e. if a small displacement analysis was used, the membrane and therefore the tensile forces would remain horizontal.

This effect is shown in Figure 3.4. It is very important to model correctly the possibility of the geosynthetic of bending and hence applying a vertical tensile force to the fill layer because, as well as the arching effect described in chapter 2, it enables the geosynthetic reinforced layer to resist vertical loads.

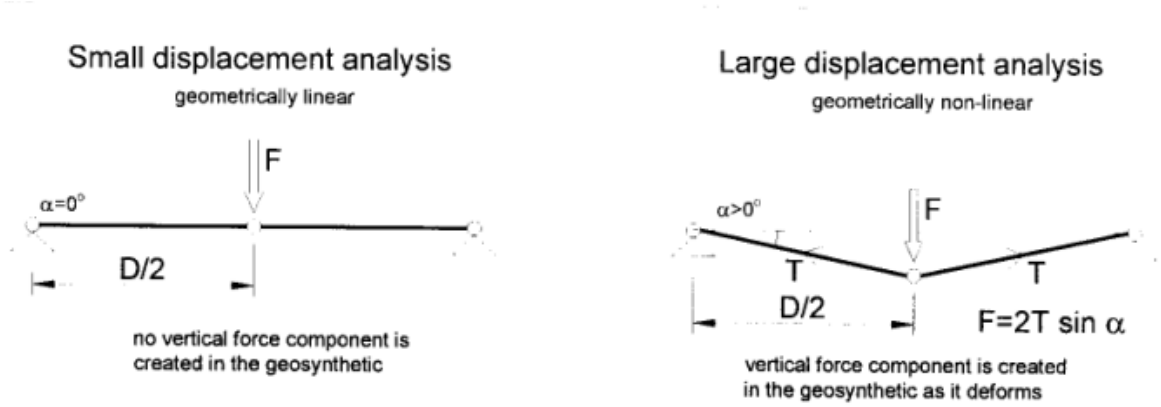

Figure 3.4: Comparison of the orientation of membrane forces in small and large displacement analyses (from Mifsud, 2005)

Chapter 4: Numerical Analysis

The first aim of the numerical analysis was to investigate the effects of the formation of a void of a particular shape directly underneath a geosynthetic reinforced fill layer. In particular, the study aims to determine the effects on the stress distribution within the fill as a consequence of the formation of a void directly beneath the geosynthetic. In Chapter 2 Terzaghi´s classical arching theory and Hewlett & Randolph´s formulation were identified as the two most suitable theories which are applicable to the case of study, and they were both described in detail.

Potts (2007) concluded that Terzaghi´s formulation was more appropriate in the case of a vertical sides void. This numerical analysis aims to determine whether this conclusion is still valid for the case on which the vertical sides of the void are inclined 45º or 60º with respect to the horizontal.

4.1 Finite Element Model

The following sections describe how the problem was modelled with the finite element method using ICFEP. The geometry of the problem, the boundary conditions and the initial stresses imposed are described in this section.

4.1.1 Geometry and Mesh

The sketches of the meshes used for the analysis of the cases in which the vertical sides of the void have an inclination of 45º and 60º with respect to the horizontal are shown on Figures 4.1 and 4.2 respectively.

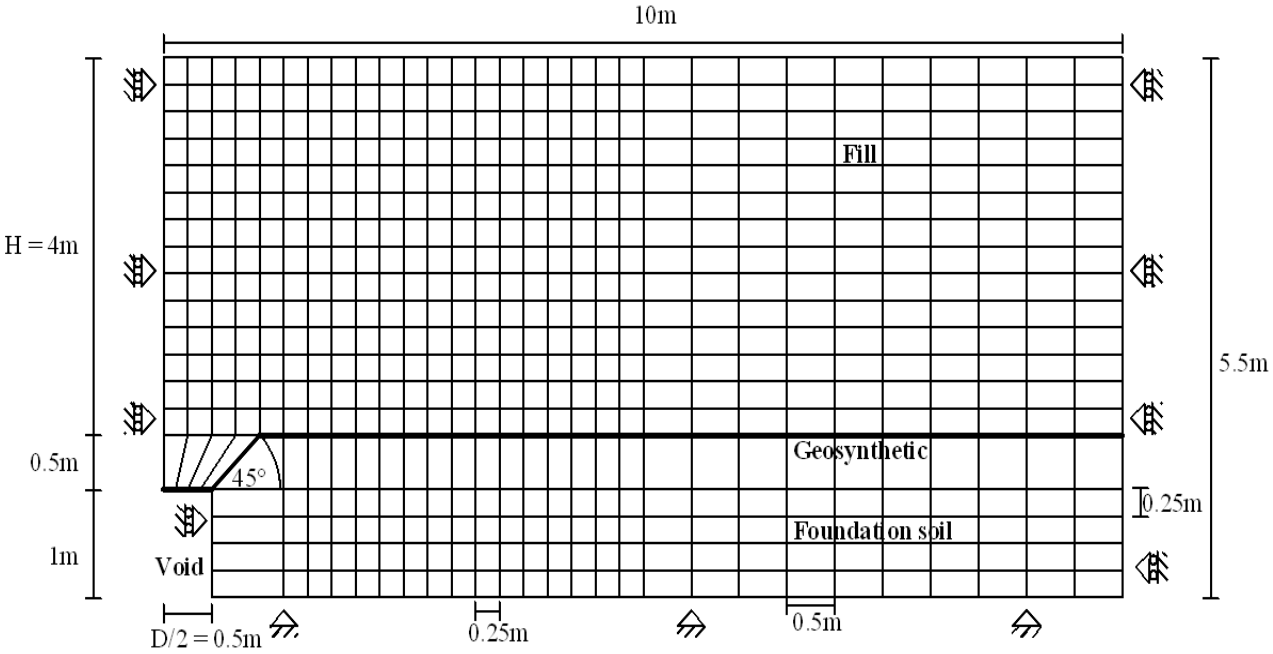

Figure 4.1: Finite element mesh and boundary conditions for the 1m wide void and 45^0 case.

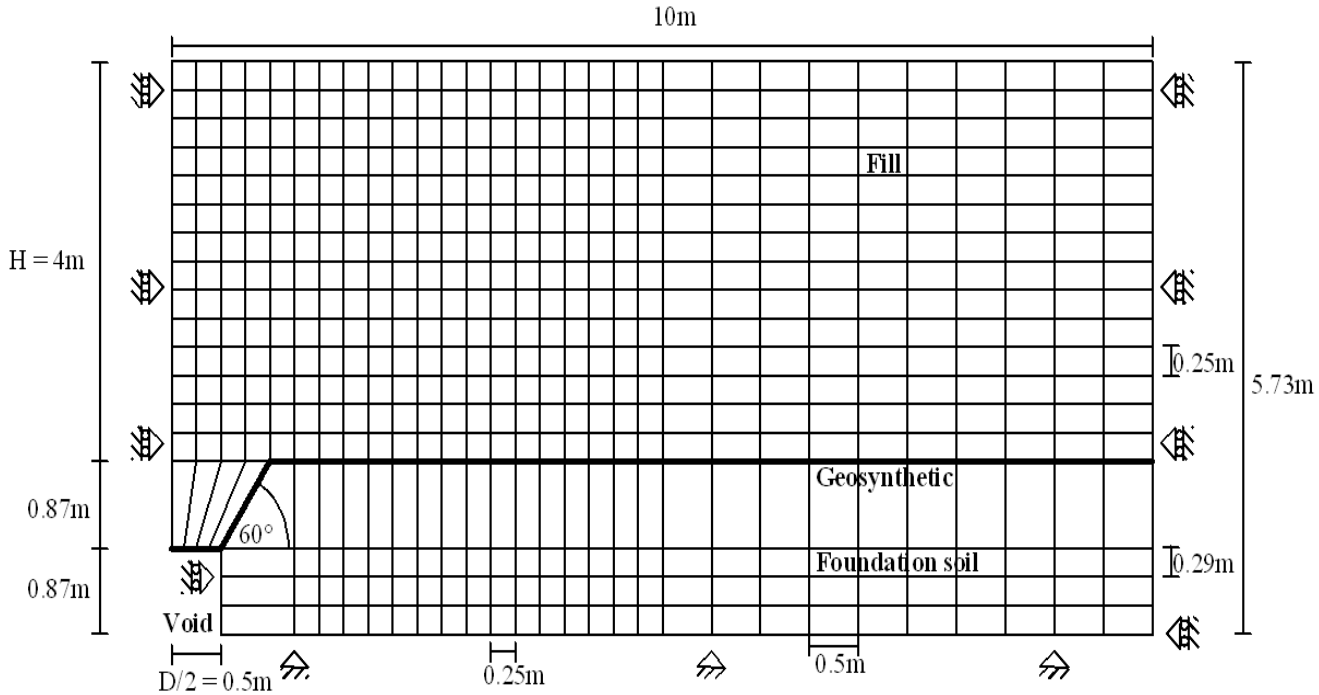

Figure 4.2: Finite element mesh and boundary conditions for the 1m wide void and 45^0 case.

Both of these meshes are for the case where a 1m wide void is formed directly beneath the geosynthetic. Only half of the problem was modelled due to the horizontal symmetry of the problem. The mesh was more refined in the fill and foundation soil directly above the void, since it is the principal area of study. The proportions of the width and the height of the overlying fill and foundation soil were chosen so as to represent the typical proportions of a low-rise construction site.

In all of the cases the height of the overlying fill was maintained to 4m, and the width D of the void varied. The fill, the geosynthetic and the foundation soil had the same properties summarized in table 2.1 for all of the analyses in this study. Of the material parameters in table 2.1 only the angle of shearing resistance of the fill was varied in section 4.2.5.

Two different void shapes were considered in this analysis:

a) Circular void, using an axisymmetric analysis.

b) Longitudinal void, using a plain strain analysis

4.1.2 Initial Stresses

In all of the analyses in this study it was assumed that the fill was completely dry, and hence the pore pressures were assumed to be zero and all of the analyses were drained. Therefore the effective stresses are equal to the total stresses in all cases. In order to simulate the effects of the real construction of the fill layer, which is described in section 4.1.4, the fill layer is initially not present. Hence the initial stresses at the geosynthetic are zero, whilst at the foundation soil these are governed be its own weight. Therefore they increase linearly with depth, being equal to $z\gamma_{soil}$, where z is the depth below the geosynthetic layer and γ_{soil} is $20kN/m^3$.

4.1.3 Boundary Conditions

The boundary conditions are represented in figures 4.1 and 4.2. In the base of the mesh all of the movements were restrained, whilst in the vertical boundaries only the horizontal movements were restrained. The vertical sides of the void were also restrained on the horizontal direction, to prevent the foundation soil from falling into the void.

4.1.4 Construction and Excavation

The process of construction of the fill layer has to be modelled with the finite element model in order to have the correct stress history in the fill material. This construction is done by layers, which for this study will be 20 cm deep. This process of construction was modelled with ICFEP in the following way.

The elements which are to be constructed are initially present in the mesh but they are initially deactivated by excavating them over increment zero of time. Then each layer of elements is reactivated to simulate its construction in stages. The construction of the fill material must be performed incrementally since superposition does not hold, even for a linear elastic material (Potts & Zdravkovic, 1999). Each layer of elements is constructed over two increments: in the first increment the layer is activated and in the next one the body forces, usually only the self weight, are applied.

The construction must be simulated in this way in a large displacement analysis to avoid the excessive deformations which would occur if the body forces are applied at the same time as the elements are activated, since the elements do not have their full strength at the beginning of the of the increment in which they are activated. Before the application of the next increment the incremental changes in stresses, displacement and strains are calculated, and the appropriate boundary conditions are applied. The excavation of the void is done in different ways, depending on the construction sequence applied, which are described in the following section.

Construction Sequences

Two different construction sequences were considered in this study:

a) Evolving void: The void is excavated beneath the geosynthetic after the process of building the fill layer by layer has ended.

b) Existing void: The void is excavated prior to the construction of the fill placed in layers on top of the geosynthetic.

The existing void sequence is useful to determine the fill height at which a stable arch forms. This height can be identified by determining the fill height at which there is no further deflection of the geosynthetic or surface settlement. Therefore this sequence is only useful for this purpose, since it does not model what could happen in reality, when a void forms after the construction of the load transfer platform.

With the evolving void sequence it is possible to find more realistic information about surface settlements, although both sequences can be used to measure the stresses and the deflections of the geosynthetic.

In the existing void sequence the void is deactivated at increment 0, and then the process of construction of the fill material is simulated. For the evolving void sequence the void is excavated after the construction process of the fill has finished, and it is done over ten

increments of time. This is done in the same way as in the numerical analyses by Potts (2007) in order to improve the convergence of the modified Newton-Raphson algorithm used in ICFEP.

The numerical analyses done by Potts (2007) proved that both sequences produced very similar results in terms of the shape of the deflected geosynthetic, the maximum deflections and the stresses for any combination of shape and size of the void. This can be seen in figures 4.3 and 4.4.

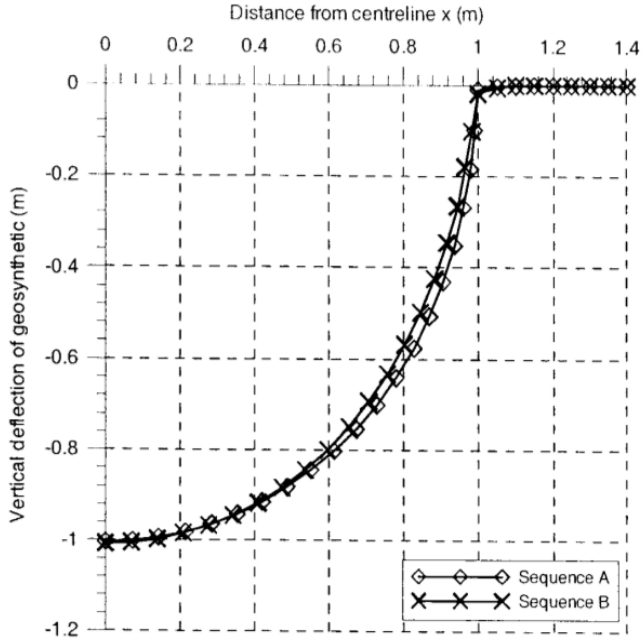

Figure 4.3: Comparison of the shape of the deflected geosynthetic using both construction sequences (from Potts, 2007)

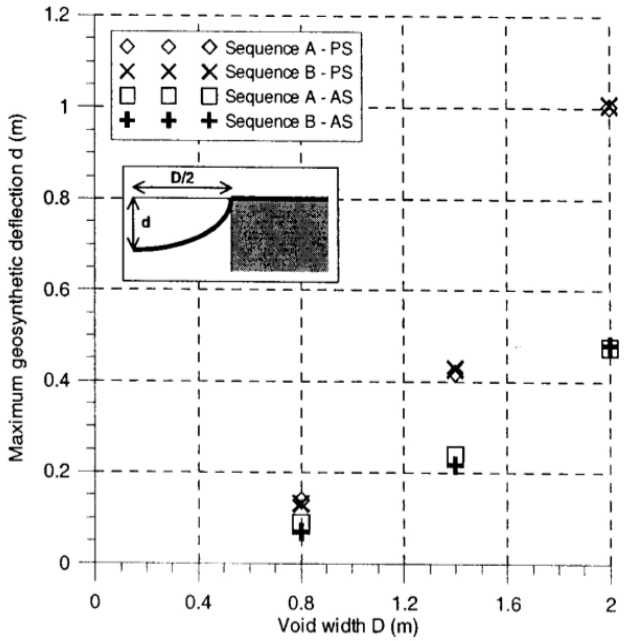

Figure 4.4: Comparison of the maximum deflections in the geosynthetic using both construction sequences (from Potts, 2007)

4.2 Analysis of the effects of the void shape

The effects on displacements and stresses on the overlying fill for different void widths and different void side inclinations for all the combinations of construction sequences (evolving void and pre-existing void) and shape (circular and longitudinal void) were analysed in this section. The void widths considered ranged from 0.5m to 3m, maintaining always a constant fill height of 4m. All of the analyses run with 4m wide voids resulted in the failure of the load transfer platform.

It was found that the formation of a circular void produced less deformations and stresses at the geosynthetic than when a plane strain void of the same width was modelled. These results agree with the results of the analysis of vertical side voids done by Potts (2007), in which it was concluded that the arching behaviour depends on the shape of the void and on the H/D ratio, and the formation of a stable arch could be expected if:

Circular void: H/D>1.5

Infinitely long void: H/D>3

Figures 4.5, 4.6, 4.7 and 4.8 show how for the case of a 1m wide void with an inclination of 45^0 of the sides of the voids with the evolving construction sequence the circular void produces smaller deflections and stresses at the geosynthetic.

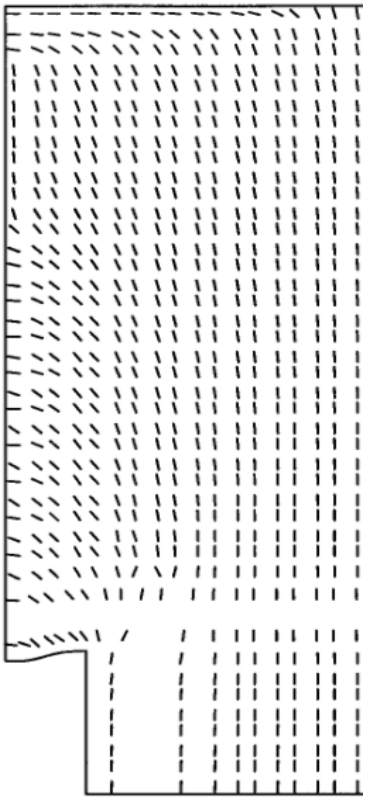

Figure 4.5: orientation of the effective for a 1m wide circular void, 45^0 case

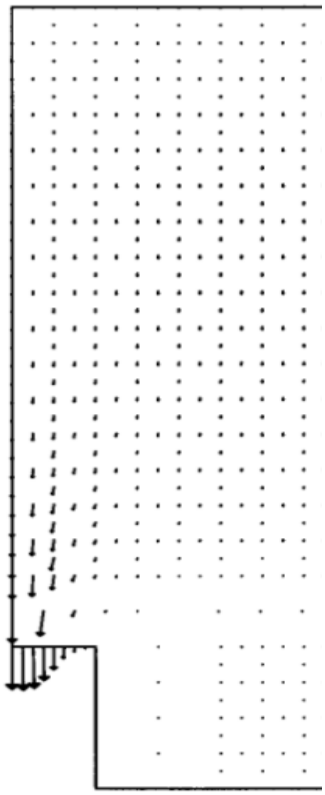

Figure 4.6: Vectors of accumulated displacement for a 1m wide circular void, 45^0 case

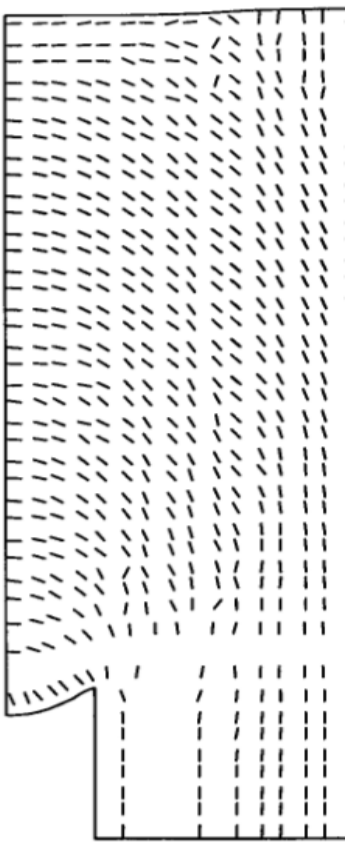

Figure 4.7: orientation of the effective for a 1m wide longitudinal void, 45^0 case

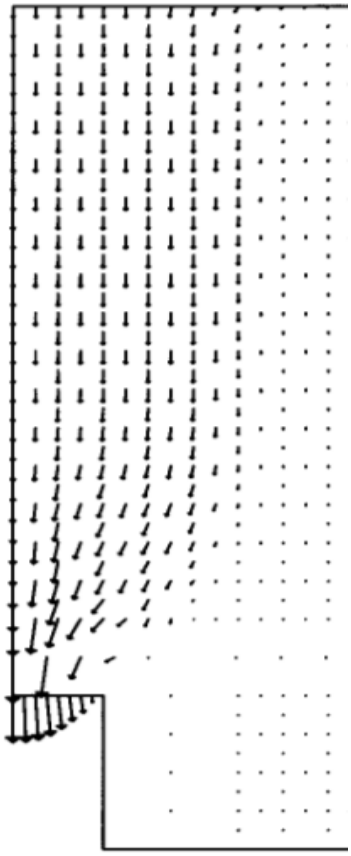

Figure 4.8: Vectors of accumulated displacement for a 1m wide longitudinal void, 45^0 case

Figures 4.6 and 4.8 represent the vectors of accumulated displacement. At each element in the mesh an arrow is generated showing the direction of the displacement. The length of the arrow represents the magnitude of the displacement, which as expected is greatest for the element right above the centre of the void.

With the circular void the maximum deflection of the geosynthetic, which occurs as we could have expected at the centre of the void, is of 71.9cm whilst with the infinitely long void it is 1.79m.

4.2.1 Vertical Stress distribution

The vertical stress profiles above the centre of the voids according to the two arching theories analysed in this study were described in chapter 2. In order to establish which if these two theories is more appropriate for the case of study the vertical stress distributions in the overlying fill immediately above the centreline of the voids were calculated for different void widths and for all the combinations of void shape and inclination of the void sides. Figures 4.9 and 4.10 show these vertical stress distributions. All of these stress distributions were computed using the evolving void construction sequence. The hydrostatic stress distribution is also represented in these plots in order to be able to determine at what depth are the stress distributions affected by the presence of the void.

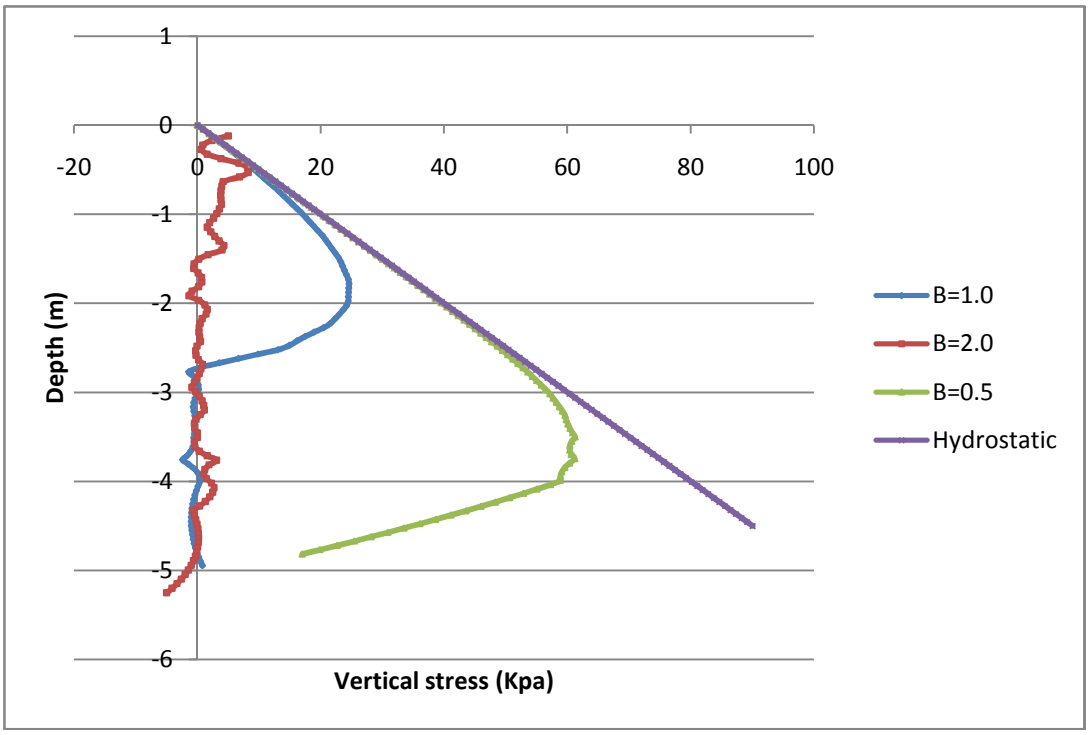

Figure 4.9: Vertical stress profile above the centreline of a circular void of different sizes with the sides inclined 60^0.

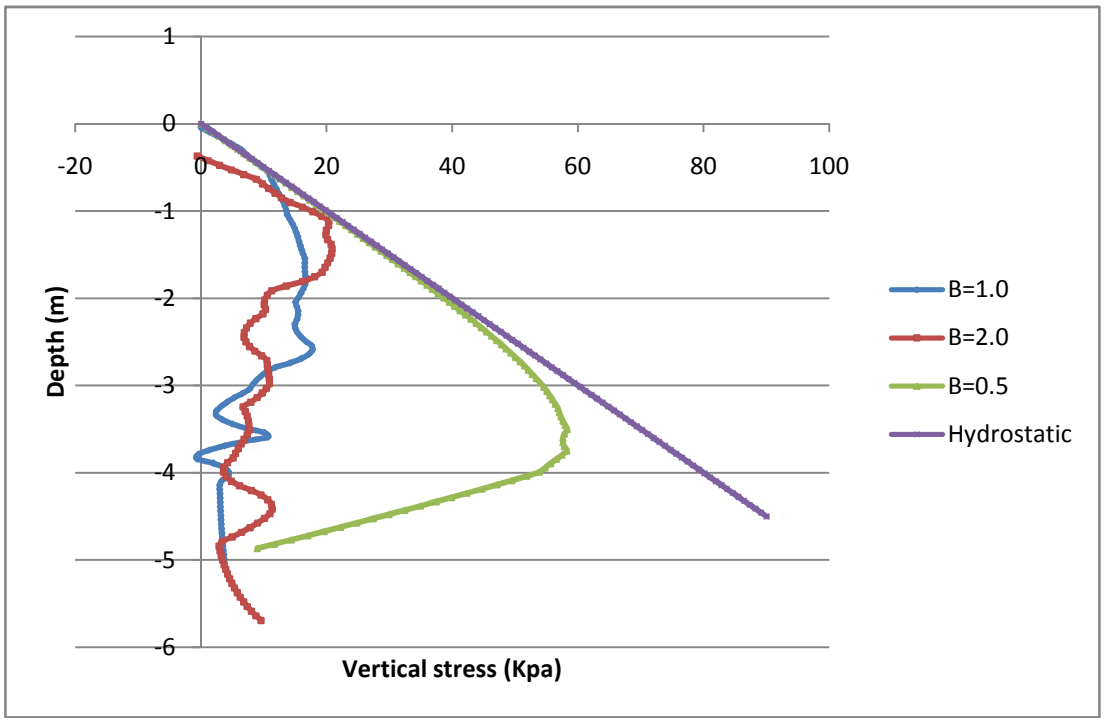

Figure 4.10: Vertical stress profile above the centreline of a longitudinal void of different sizes with the sides inclined 60^0.

For both the circular and longitudinal voids for the 60^0 case the disturbed fill was propagated to the surface for void widths bigger than 2m. For the 1m void a stable arch is formed in the fill over a circular void but not over a longitudinal one. The formation of a stable arch was achieved for lower H/D ratios for circular voids than for longitudinal ones in all of the cases

analysed in this study.

For the cases in which the disturbed fill is propagated to the surface it was already established that Terzaghi's Classical arching theory is more appropriate. The question which needs to be clarified is the case in which a stable arch is formed above which the soil is undisturbed.

In this case in the stress profile is initially very similar to the hydrostatic profile, but then at some critical height H_c the stresses start to decrease. This indicates that the stresses are being transferred into the surrounding soil, and therefore the arching behaviour can be identified. This height is of approximately 1.1m for the circular void and 1.5m for the infinitely long void when the void width is 0.5m. For the circular void width of 1m this critical height is approximately 2.2m. These results suggest that, when the sides of the voids are inclined 60^0 with respect to the horizontal, a stable arch can be expected if:

- Circular void: H/D>2.2
- Infinitely long void: H/D>3

Similar results in terms of the critical height and the vertical stress profiles were obtained for the 45^0 case. Figure 4.11 shows that the vertical stress profile in the fill above a longitudinal void for the 45^0 case is very similar to the 60^0 case, shown in Figure 4.10. In both of them, a stable arch could only be identified in the case of a 0.5m wide void.

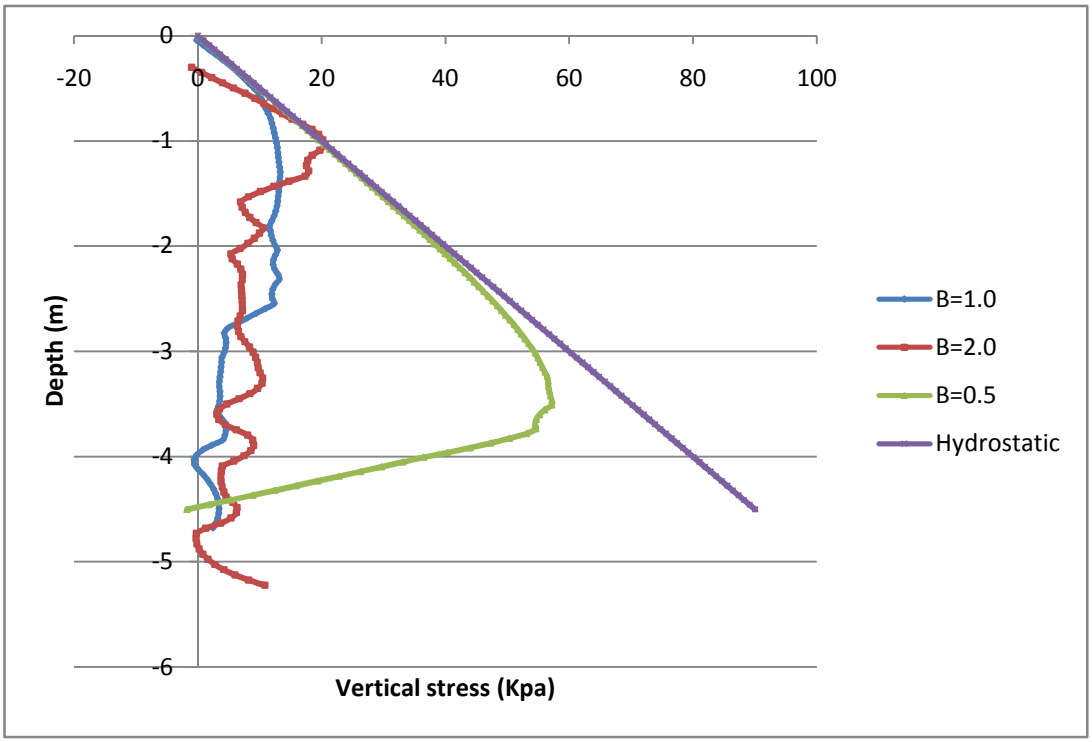

Figure 4.11: Vertical stress profile above the centreline of a longitudinal void of different sizes with the sides inclined 45^0.

The vertical stress profiles for both the 45^0 and 60^0 cases do not differ substantially from

those found by Potts (2007) when considering voids with vertical sides. The vertical stresses do not increase beneath the soil arch as predicted by Hewlett & Randolph's formulation, but instead they continue to decrease. Therefore it seems reasonable to assume that Terzaghi's theory is still the most appropriate one also when the sides of the void have a certain inclination. This conclusion can be corroborated by considering the orientation of the major principal stresses in the fill, which are analysed in the following section.

4.2.2 Orientation of the major principal stresses

Terzaghi's approach considers the formation of a shear surface rising from the edges of the void upwards through the fill, with a slight inclination. On the other hand, Hewlett & Randolph's approach proposes the formation of a physical arch which spans across the void. In this latter case the major principal stresses should be tangential to this arch.

Therefore another way of determining which of the two theories is more appropriate is by considering the plots of the orientation of the major principal stresses for the cases in which there is still some doubts regarding which is more suitable, i.e, when a stable arch is formed.

Figures 4.13 and 4.14 show the orientation of the major principal stresses above a 1.0 wide longitudinal void and over a circular void respectively, for a fill constructed over a pre-existing void. The inner radius of the soils arch in Hewlett & Randolph's formulation is D/2, which in this case would be 0.5m. To determine the outer radius the vertical stress profiles need to be calculated for both cases, which are shown in Figure 4.12.

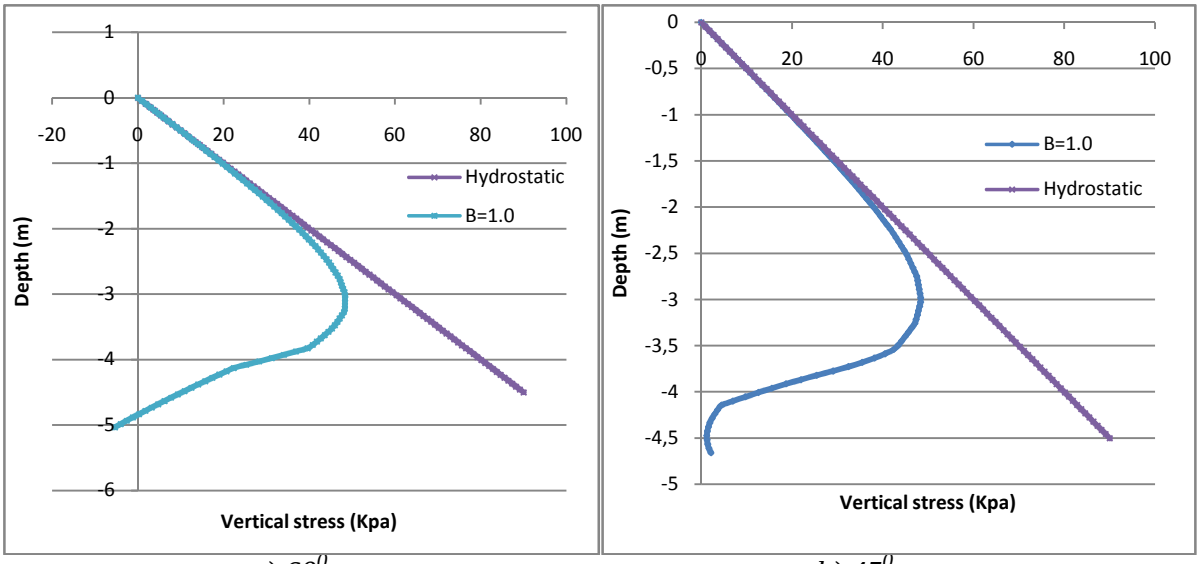

a) 60^0 case *b) 45^0 case*

Figure 4.12: Vertical stress profile above the centreline of a longitudinal void with different inclinations of the vertical boundaries.

The maximum vertical stress was of 48.4Kpa and occurred at a height of approximately 1m above the void, for both cases. This height would correspond to the outer radius of the soil arch in Hewlett & Randolph's formulation.

According to Hewlett and Randolph's approach the orientation of the major principal stresses should be tangential to the arches at all of the points within the inner and outer radius. In the cases considered, although the stresses are not exactly tangential at all points it still seems to be a quite reasonable approximation for the orientation of the principal stresses.

The results displayed in Figures 4.13 and 4.14 suggest that the true width if the soil arch is actually larger than what was predicted by considering the height at which the maximum vertical stresses occurs. It seems that this width corresponds to the length of the inclined side of the void. The soil arches corresponding to these widths have also been sketched on Figures 4.13 and 4.14 .This would be a very logical assumption since Hewlett & Randolph's formulation was proposed for a piled embankment in which the width if the soil arch corresponded to the whole width if the soil caps, and the inclined side of the void provides a similar support for the soil arch as the pile caps. This possibility was further investigated by considering the orientation of the major principal stresses for voids of different widths.

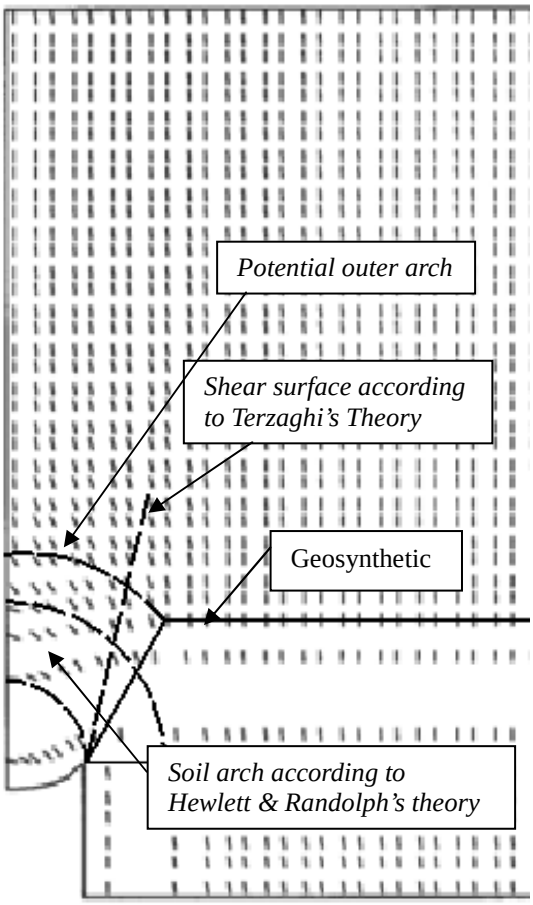

Figure 4.13: Orientation of the major stresses above a 1.0 wide longitudinal void for the 60^0 case

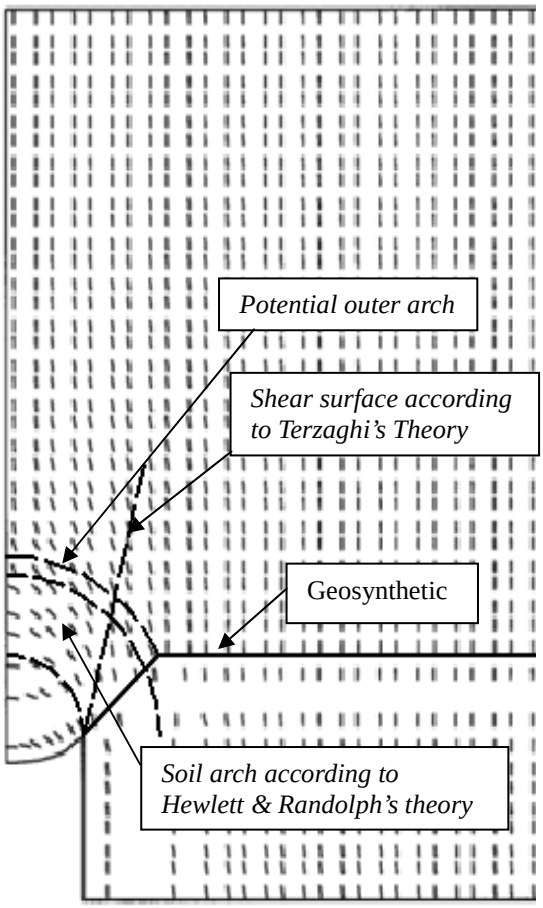

Figure 4.14: Orientation of the major principal stresses above a 1.0 wide circular void for the 45^0 case.

The case of a 2m wide longitudinal void with its sides inclined 60^0 and that of a 0.5m wide longitudinal void with its sides inclined 45^0 are shown on Figures 4.15 and 4.16 respectively. In the first case the maximum vertical stress occurred at a height of 1.9m above the void, and in the second case at a height of 1m. These heights correspond to the theoretical outer radius of the soils arches proposed in Hewlett & Randolph's formulation, and sketched on the corresponding figures.

As well as for the case of a 1m void, the orientation of the major principal stresses are quite

close to being tangential to the arches proposed in Hewlett & Randolph's theory. The width of this soil arch can again be approximated by the length of the inclined part of the foundation soil.

.

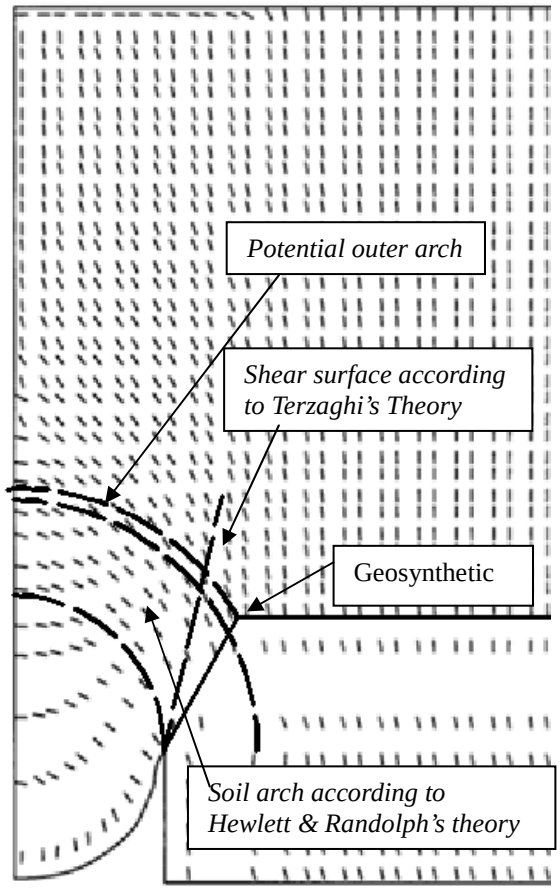

Figure 4.15: Orientation of the major principal stresses above a 2.0m wide longitudinal void for the 60^0 case

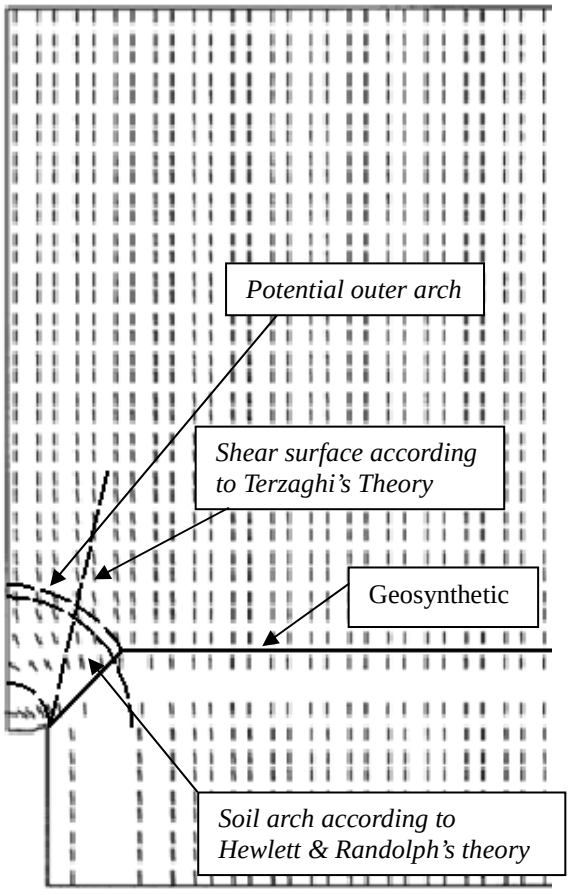

Figure 4.16: Orientation of the major principal stresses above a 0.5m wide longitudinal void for the 45^0 case

Hence it seems that Terzaghi's approach is more appropriate in terms of predicting the vertical stress profile in the overlying fill, but with Hewlett & Randolph's formulation the orientation of the major principal stresses can be predicted more accurately, by adopting the length of the inclined part of the foundation soil as the width of the soil arch proposed in this formulation.

4.2.3 Maximum deflections of the Geosynthetic

The maximum deflections of the geosynthetic as well as the shape of the deformed geosynthetic were analysed for the cases in which the sides if the void are inclined 45^0 and 60^0. In the previous section it was seen that there are not any substantial differences between these two cases in terms of the vertical stress distribution or the orientation of the major principal stresses. The maximum geosynthetic deflection occurred, as expected, at the centre of the void for all of the cases analysed. The values of the maximum geosynthetic deflection above voids of different combinations of widths and inclination of the sides of the void are shown in Figure 4.17, all of them with the evolving construction sequence and for both a circular and a longitudinal void.

It can be seen from these figures that the maximum geosynthetic displacement is almost identical for the cases of the 45^0 and 60^0 sides voids of small widths, for both a circular or a longitudinal void. Only when considering void widths of 2m wide a slight difference in the geosynthetic deflection can be appreciated. In these latter cases, the geosynthetic deflection at the centre of the void is larger for the 60^0 case.

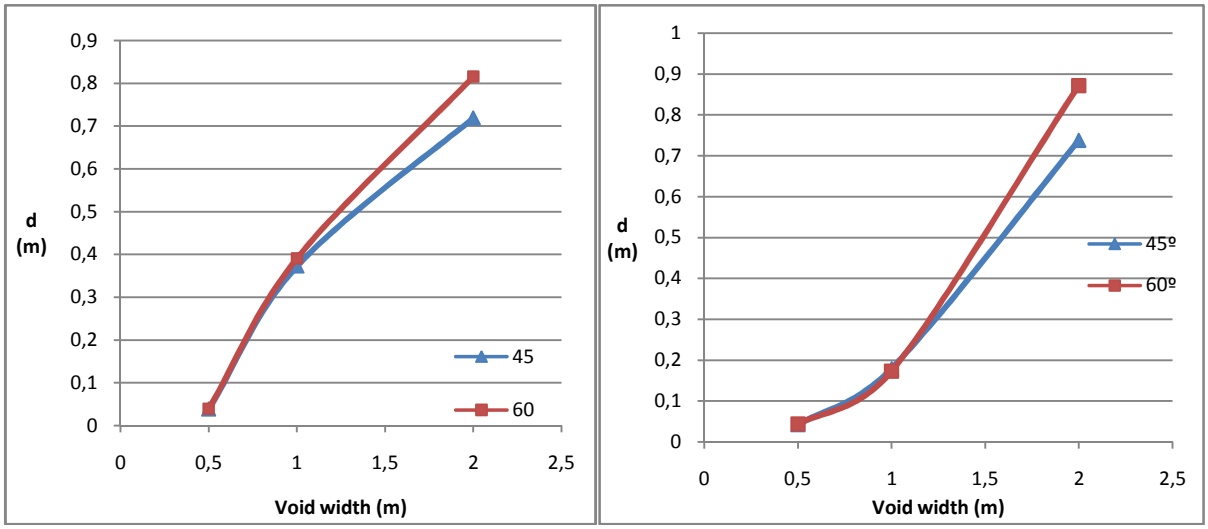

a) Circular void *b) longitudinal void*

Figure 4.17: Maximum geosynthetic displacement above voids of different width, shape and void sides inclinations, with the evolving construction sequence.

The same conclusions can be extracted by analysing the case in which the overlying fill is constructed above a pre-existing void. Figure 4.18 shows the values of the maximum geosynthetic deflection above voids of different combinations of width, shape, and inclination of the sides of the void using existing construction sequence.

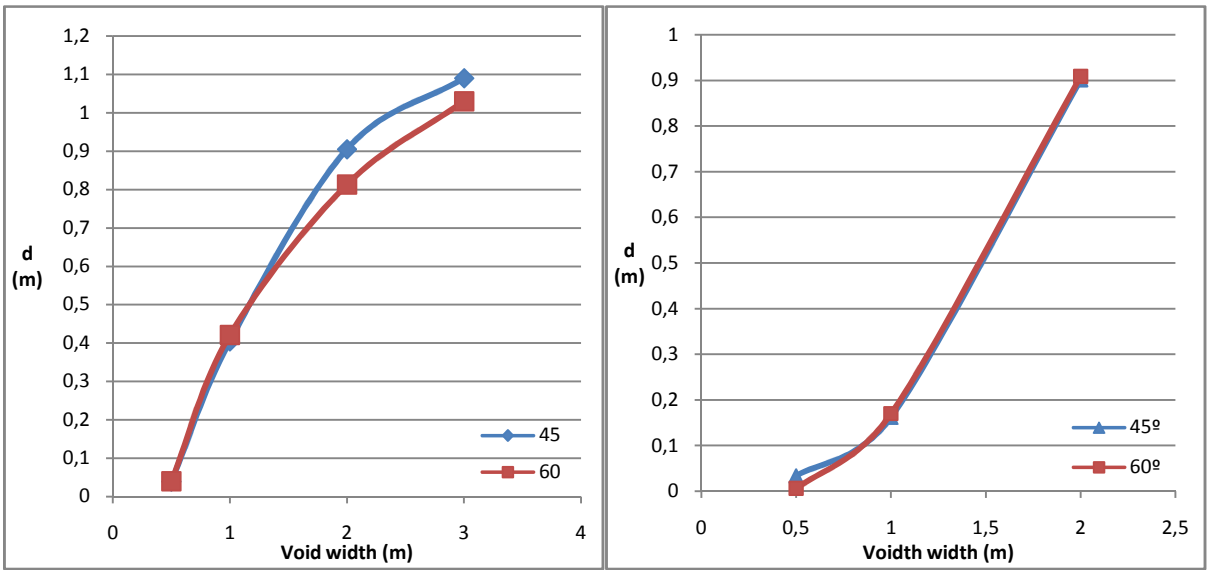

a) Circular void *b) longitudinal void*

Figure 4.18: Maximum geosynthetic displacement above voids of different width, shape and void sides inclinations, with the existing construction sequence.

Once again the maximum deflections of the geosynthetic are fairly similar for both inclinations. In the last section it was seen that the vertical stress distributions were also quite similar for the two different void side inclinations. Therefore it seems that the inclination of the vertical boundaries of a void which forms beneath the geosynthetic layer of a load transfer platform does not have a significant effect on the deformations and stresses of the geosynthetic.

4.2.4 Shape of the deflected geosynthetic

For the case of a vertical sides void forming beneath a geosynthetic reinforced embankment it was seen in Chapter 2 that the shape of the deflected geosynthetic could be approximated by a circular arch. This implies that there is a non-zero horizontal stress at the level of the geosynthetic, which from the plots of the orientation of the major principal stresses we know is true. Figures 4.19 and 4.20 show the deflections of the geosynthetic above a void for different combinations of void widths and shapes for the case in which the vertical boundaries of the void have an inclination of 45^0 and 60^0 respectively.

The displacement of the geosynthetic is normalised by the maximum displacement, which always occurred at the centre of the void, and the distance from the centre of the void was normalised by the half width of the void. This enables the comparison of the shape of the deflected geosynthetic for different void widths.

The shapes of the deflected geosynthetic are fairly similar for the different void widths, particularly for the longitudinal voids. In the case of a circular void the shapes differ more from each other, since the deflections start to decrease at a shorter distance from the centre of the void for the smaller voids.

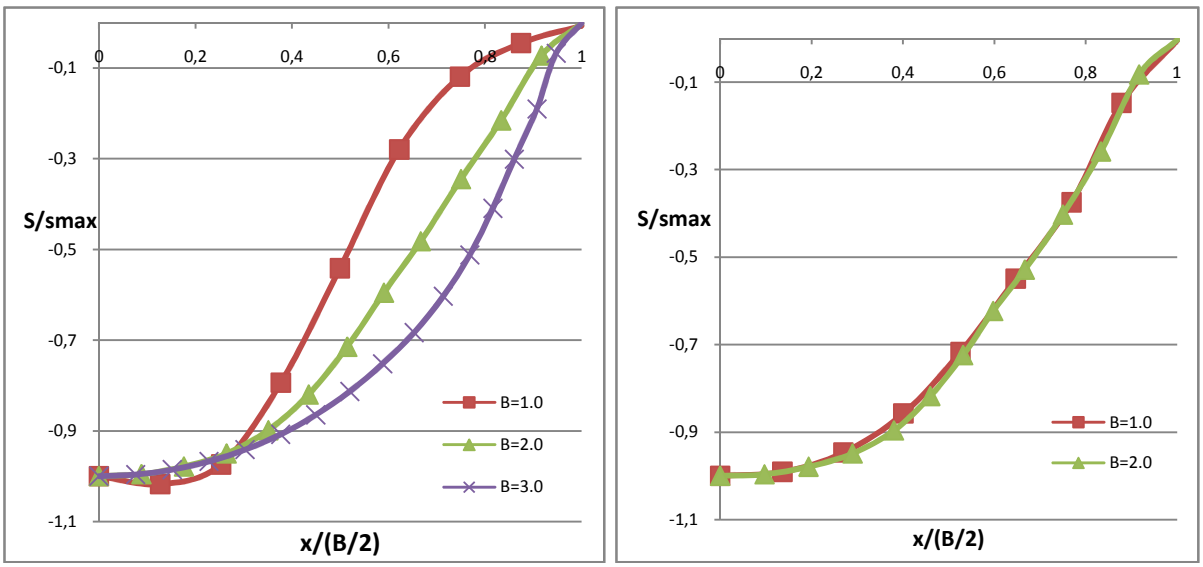

a) Circular void *b) Longitudinal void*

Figure 4.19: Shape of the deflected geosynthetic above a circular and longitudinal void of different sizes for the 45^0 case.

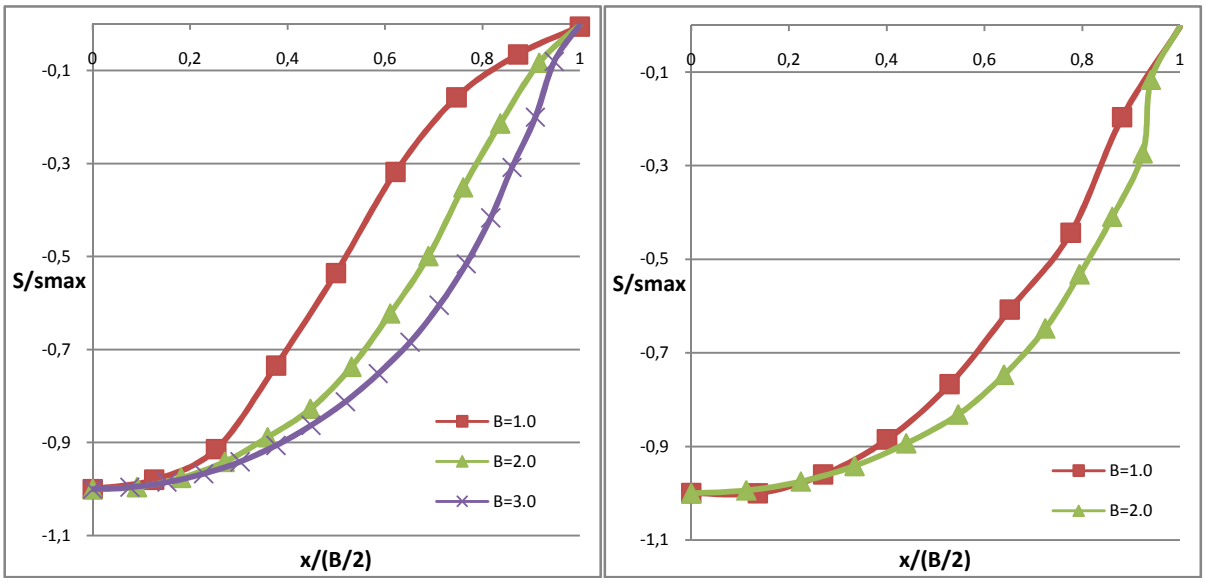

a) Circular void *b) Longitudinal void*

Figure 4.20: Shape of the deflected geosynthetic above a circular and longitudinal void of different sizes for the 60^0 case.

Once again there are no appreciable differences in the behaviour of the fill layer and the geosynthetic between the 45^0 and 60^0 cases, since the plots of the deflected geosynthetic are quite similar for both cases. Hence it can be concluded that the inclination of the vertical sides of the void does not have a relevant effect on the overall behaviour of the system.

In the case of the longitudinal void, when the void width was 3m the fill layer failed and collapsed into the void, and hence non convergent results were obtained. In all of the analyses the circular voids produced smaller stresses and deflections of the geosynthetic, and wider voids could be supported. An example of how the finite element analysis models the failure when a 3m wide longitudinal void is formed beneath the geosynthetic is shown in Figure 4.21.

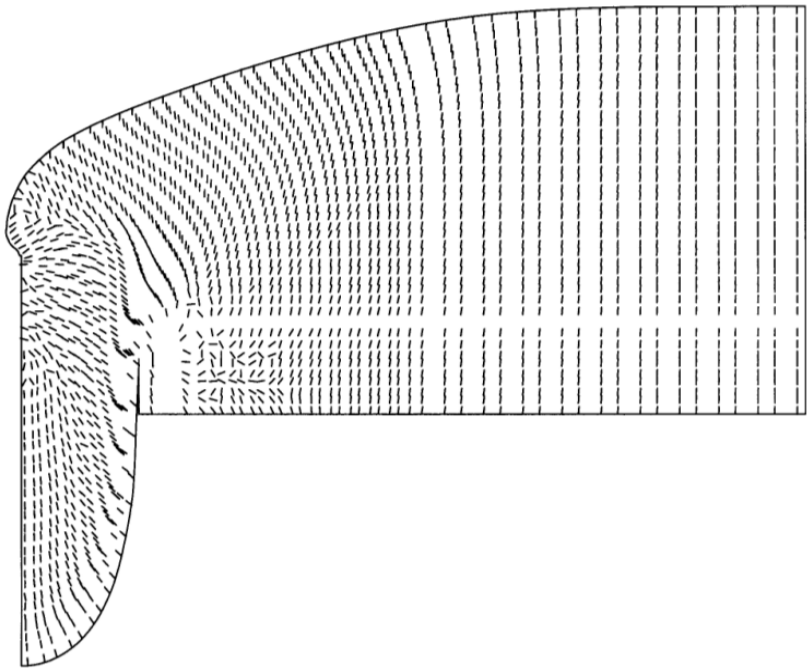

Figure 4.21: Failure of the platform above a 3m wide longitudinal void

The two most appropriate shapes for approximating the real shape of the deflected geosynthetic are the parabolic arc and the circular arc. These shapes can be constructed through the points defined by the maximum geosynthetic deflection d and the void width D using the equations 4.1 and 4.2. Figures 4.22 and 4.23 show the sketches of the deformed geosynthetic when they are approximated by a parabola and a circular arc respectively, showing the coordinate system used and the parameters used in the equation describing these shapes. x is the distance from the centre of the line and y the vertical distance from the undeformed position of the geosynthetic.

Parabolic arc:

$$y = -4\frac{dx^2}{D^2} + d \tag{4.1}$$

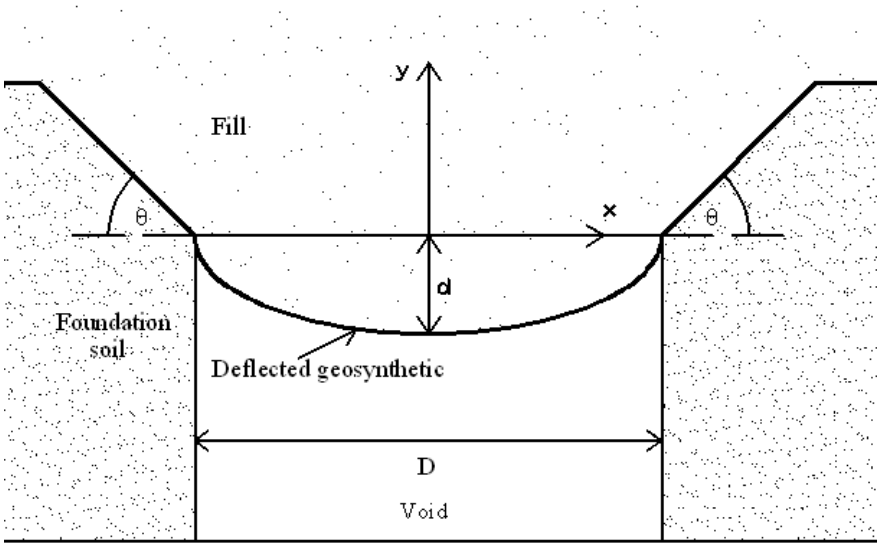

Figure 4.22: Sketch of the deflected geosynthetic approximated by a parabola

Circular arc:

$$x^2 + (y + r - d)^2 = r^2, \text{ where } r = \frac{d}{2} + \frac{D^2}{8d} \tag{4.2}$$

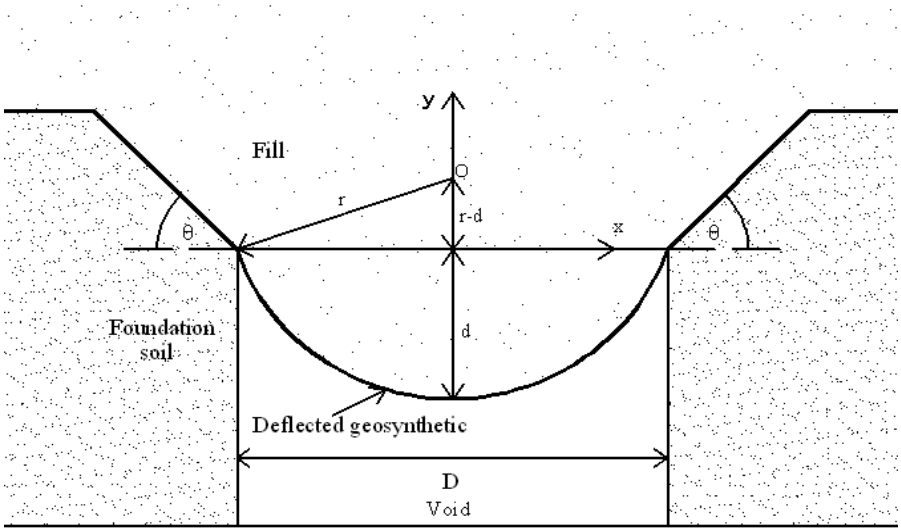

Figure 4.23: Sketch of the deflected geosynthetic approximated by a circular arc

The deflections of the geosynthetic above a longitudinal void of different combinations of widths and inclination of the vertical boundaries were computed using the finite element model with ICFEP. The resulting shape of the deflected geosynthetic is compared with the parabolic and circular arcs calculated using equations 4.1 and 4.2 respectively, and these are shown on Figures 4.24 and 4.25.

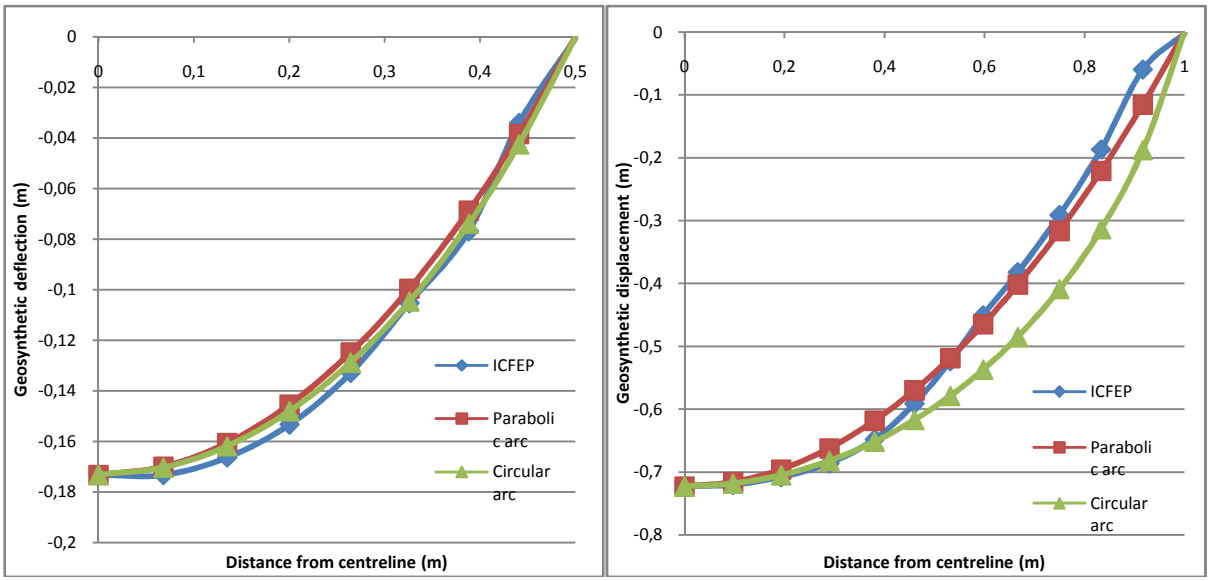

a) D = 1.0m b) D = 2.0m

Figure 4.24: Comparison of the shape of the deformed geosynthetic with the parabolic and circular arcs, above a longitudinal void of different widths for the 45^0 case.

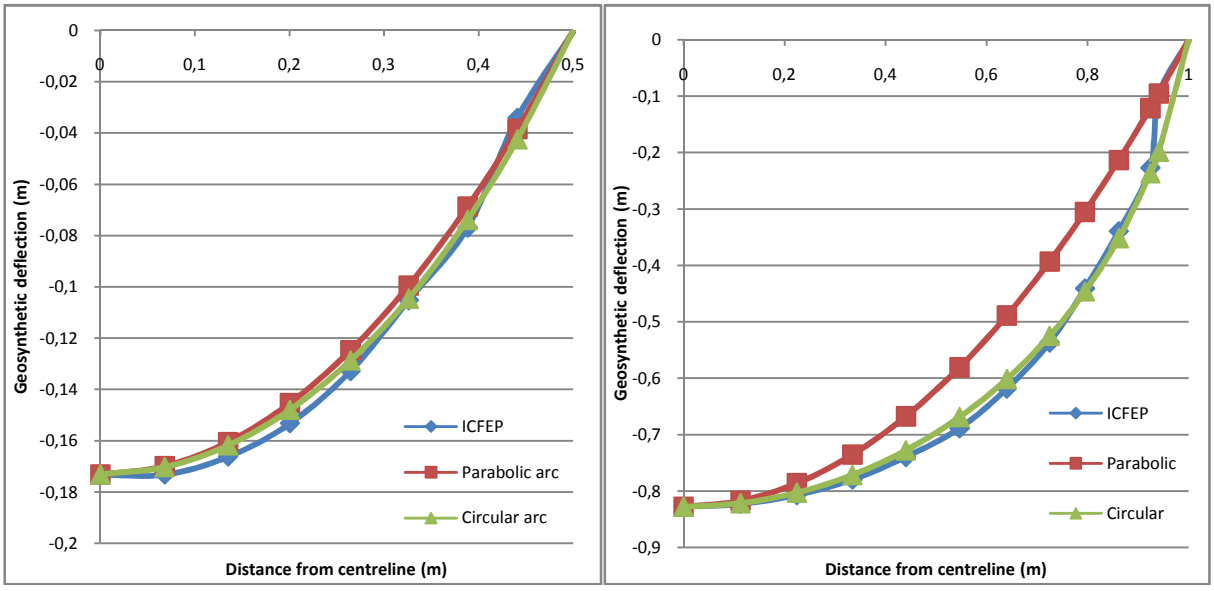

a) D = 1.0m b) D = 2.0m

Figure 4.25: Comparison of the shape of the deformed geosynthetic with the parabolic and circular arcs, above a longitudinal void of different widths for the 60^0 case.

For the case of a 1m wide void both the parabolic and circular arcs under predict the geosynthetic displacements, although the circular arc is closer to the shape of the deflected geosynthetic predicted by the finite element model. In the case of a 2m wide void the

displacements predicted by the parabolic arc are significantly smaller than those predicted by ICFEP, and the circular arc provides a better match. In any case, it is clear that the shape of the deflected geosynthetic above a void with inclined vertical boundaries can be approximated by a circular arc. This confirms the results obtained by Mifsud (2005), who concluded that the circular approximation was more realistic for the case of a vertical boundaries void.

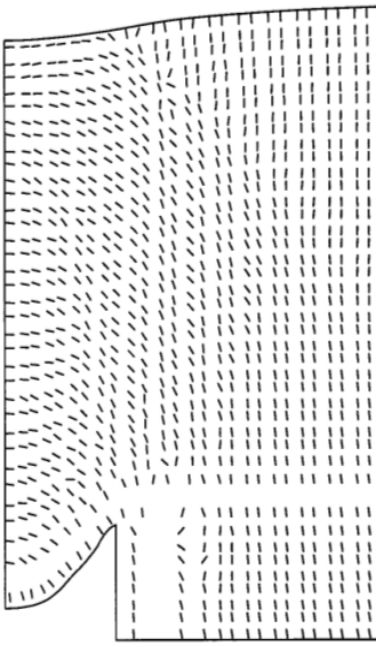

Figure 4.26: Orientation of the major principals stresses above a 2m wide longitudinal void

Since the pressure acting on the geosynthetic must be normal to it, the fact that the shape of the deflected geosynthetic can be approximated by a circular arc means that there is a non-zero horizontal component of the stress at the level of the geosynthetic. This means that there is some load transfer mechanism developed in the fill which sheds loads into the surrounding fill. This is true even when a stable arch is not formed, as in the case of a 2m wide longitudinal void where it can be seen from the plot of the orientation of the major principal stresses shown in Figure 4.26 that the disturbed fill is propagated to the surface.

4.2.5 Effect of the variation of the angle of shearing resistance.

In chapter two it was seen that increasing the angle of shearing resistance of the overlying fill enabled the formation of a stable soil arch across the void and hence the stresses and the deflections at the level of the geosynthetic were reduced, for the case of voids with vertical boundaries. Since the results in the previous sections of this chapter proved that the behaviour of the system is fairly similar for the cases in which the vertical boundaries have an inclination of 45^0 or 60^0, the analyses of the effect of the angle of shearing resistance were all done for the 45^0 case.

The cases of a void of different widths and shapes forming beneath a geosynthetic reinforced platform with values of the angle of shearing resistances of the overlying fill ranging from 25^0 to 45^0 are analysed in this section. A fill with an angle of shearing resistance of 25^0 would be possible with a high plasticity clay, whilst a φ'_{fill} of 45^0 could be achieved using a very dense granular soil. The maximum geosynthetic deflections above a 2m and a 1m wide void of different shapes and different φ'_{fill} are shown on Figure 4.26.

These results confirm that the formation of a longitudinal void simulated using a plain strain analysis produces greater maximum geosynthetic deflections than if a circular void of the same width was formed. It is also clear that, as expected, the greater angle of internal shear resistance of the fill the lower the maximum geosynthetic deflections and stresses at the level of the geosynthetic. This reduction in the maximum geosynthetic displacement is greater for

longitudinal voids than for circular voids.

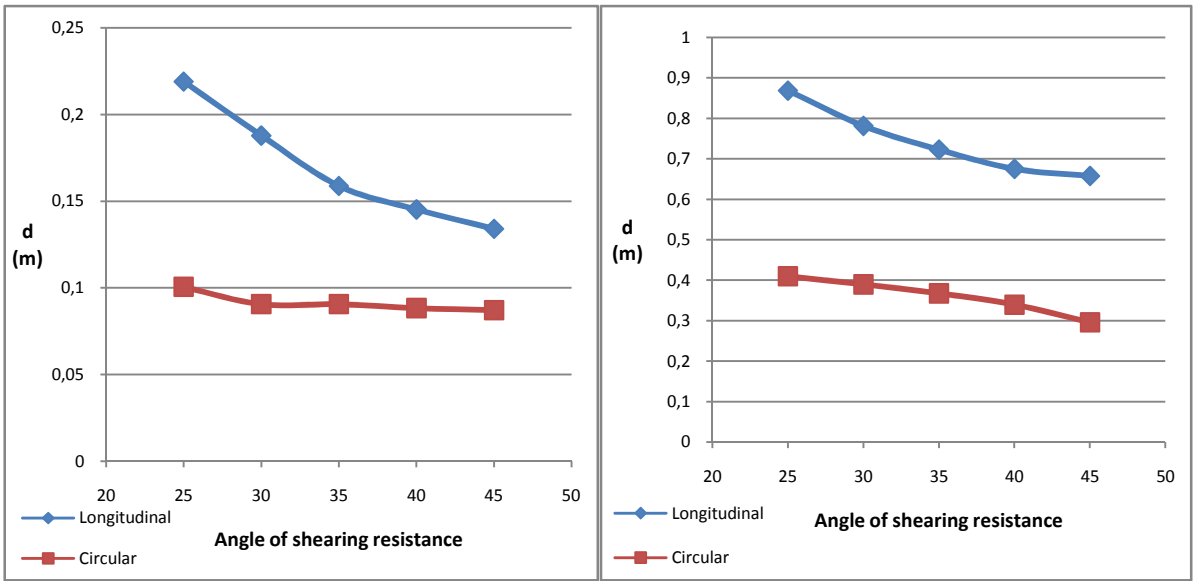

a) D = 1m *b) D = 2m*

Figure 4.26: Maximum geosynthetic deflections above a void of different widths and a varying φ'_{fill} with the evolving construction sequence

Figure 4.27 shows the vertical displacements of all the points of the geosynthetic directly above a 1m and a 2m wide void, for the case of a longitudinal void. This figure clearly illustrates the effect of the angle of shearing resistance of reducing the vertical geosynthetic displacements of all the points directly above the longitudinal void. Similar results were obtained for the case of a circular void.

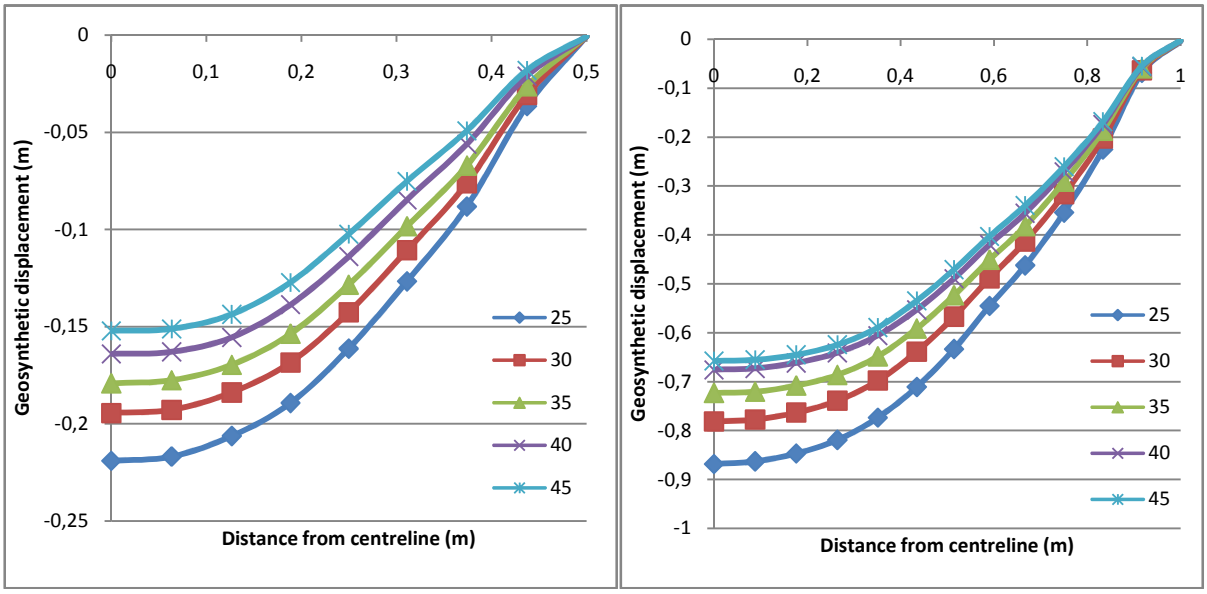

a) D = 1m *b) D = 2m*

Figure 4.27: Geosynthetic deflections above a longitudinal void of different widths and a varying φ'_{fill} with the evolving construction sequence

The shapes of the deflected geosynthetic are very similar for all the different values of the angle of shearing resistance, especially for the 2m wide void case. This can be seen in figure 4.28, where the vertical displacements have been normalised by the maximum displacement

and the distance from the centreline by half of the void width.

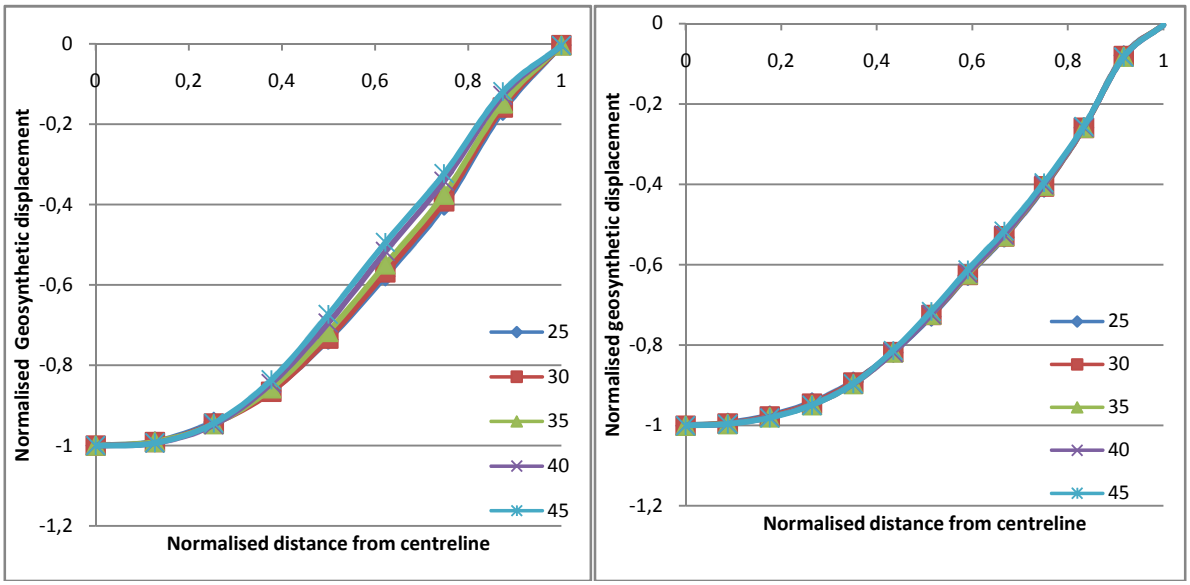

a) D = 1m *b) D = 2m*

Figure 4.28: Normalised shape of the deflected geosynthetic above a longitudinal void of different widths and a varying φ'_{fill} with the evolving construction sequence

The shapes of the deflected geosynthetic are almost identical for the case of a 2m wide void, whilst for the 1m wide void there are very small differences in the shape of the deflected geosynthetic, resulting in slightly steeper inclinations of the geosynthetic for higher values of the angle of shearing resistance.

For all the cases it was seen that the approximation of a circular arch for the shape of the deflected geosynthetic produced a better match than the parabolic arch, since the latter one underestimated the deflections in the central area of the void. Hence it can be concluded that the angle of shearing resistance of the fill does not have a noticeable influence on the shape of the deflected geosynthetic.

The reduction in the geosynthetic displacement is due to the formation of a load transfer mechanism which sheds the load on the surrounding soil hence reducing the pressure on the geosynthetic. This mechanism can be seen by observing the orientation of the principal stresses within the fill. Figures 4.29 and 4.30 show these plots for the cases of a 1m and a 2m wide void respectively.

For both the 1m and 2m wide void cases a more stable and compact soil arch can be identified from these plots when the angle of shearing resistance of the fill is greater. When $\varphi'_{fill} = 45^0$ a greater depth of the overlying fill is unaffected by the presence of the void, and hence a more effective load transfer mechanism is developed. Therefore it is highly desirable to build the load transfer platform with a high φ'_{fill}, since this reduces the stresses and the deflections of the geosynthetic.

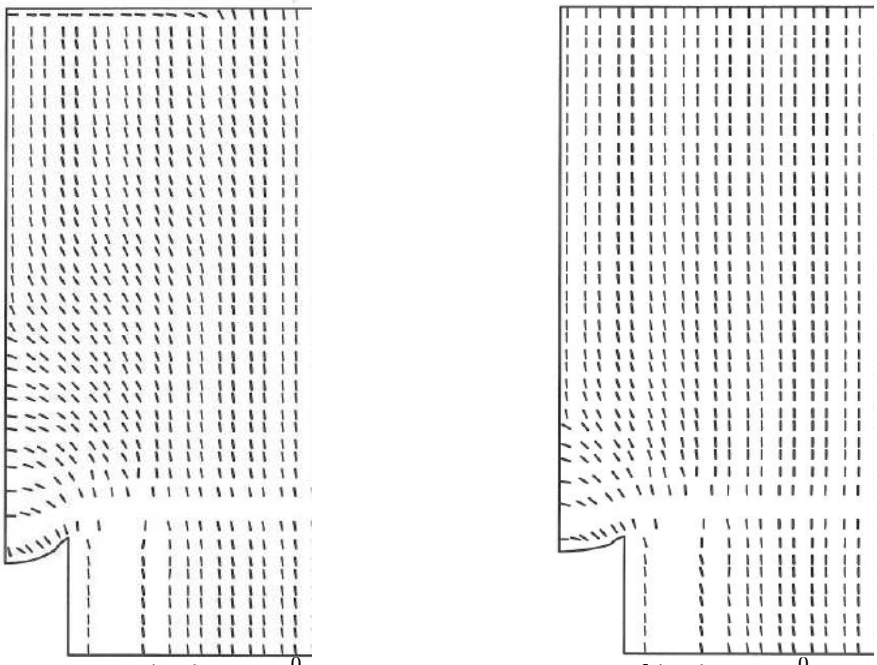

a) $\varphi'_{fill} = 25^0$ b) $\varphi'_{fill} = 45^0$

Figure 4.29: Orientation of the major principal stresses in the fill above a 1m wide longitudinal void, with different values of φ'_{fill}

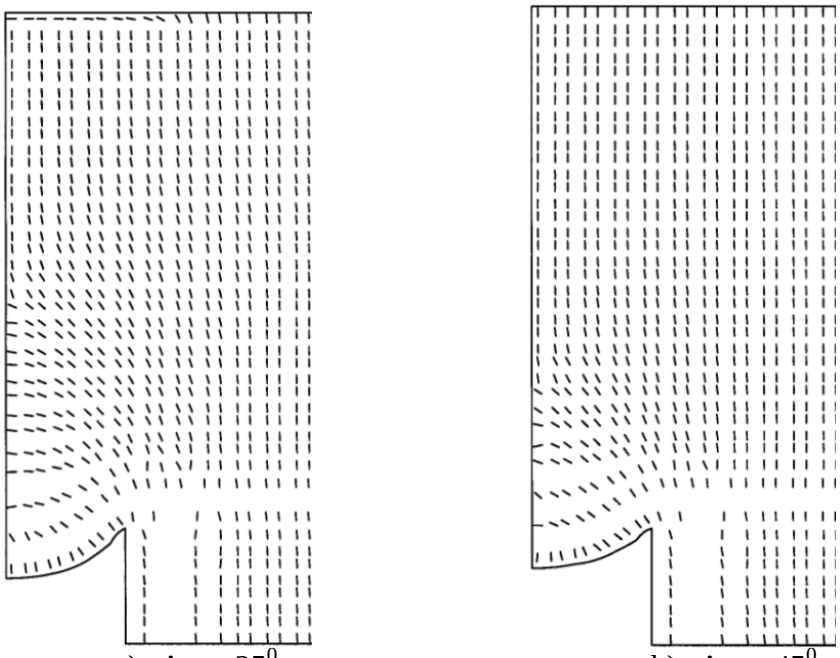

a) $\varphi'_{fill} = 25^0$ b) $\varphi'_{fill} = 45^0$

Figure 4.30: Orientation of the major principal stresses in the fill above a 2m wide circular void, with different values of φ'_{fill}

4.2.6 Compaction Properties

In all of the analyses done so far it was assumed that the overlying fill material was completely dry. The aim of this section is to model the effects that the soil suction in the fill may have on the arching behaviour when a void is formed beneath the geosynthetic.

The load transfer platform was modelled using ICFEP with three different values of the soil suction: 10, 20 and 30 Kpa. As well as in the previous section, all of the analyses were done for the case in which the vertical boundaries of the void have an inclination of 45^0. The orientation of the major principal stresses in the fill above a 2m wide longitudinal void are shown in Figure 4.31, for two different values of the suction.

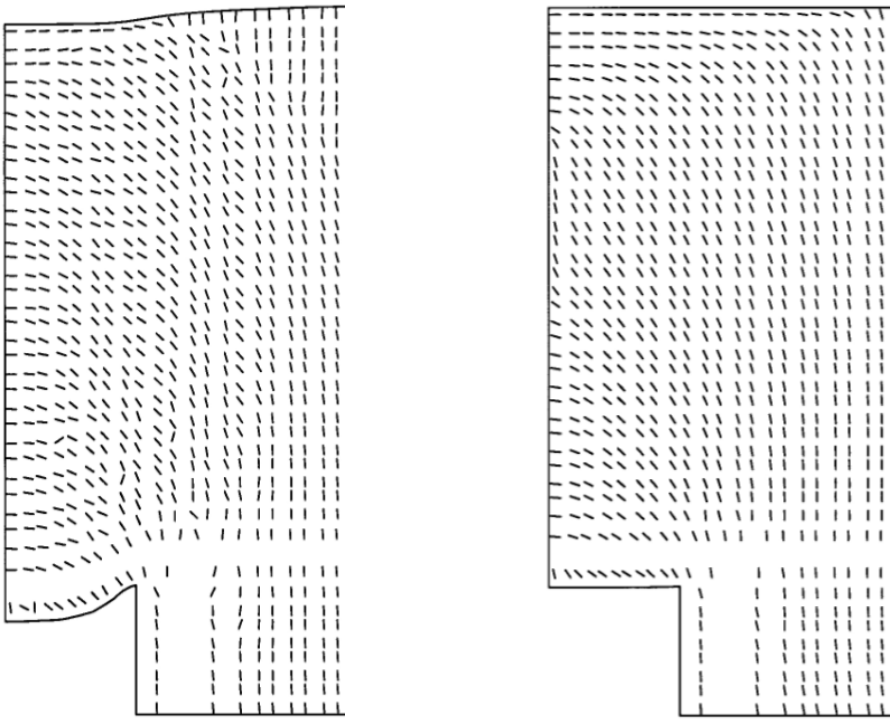

a) Suction = 10Kpa *b) Suction = 30Kpa*

Figure 4.31: Orientation of the major principal stresses above a 2m wide longitudinal void for the 45^0 case and for different values of suction.

It can be seen in this figure that when the suction is 10Kpa the area of the fill which is affected by the presence of the void is propagated to the surface and the lateral extent of the disturbed fill is greater than when the suction is 30KPa. A more clear and stable arch can be identified when the suction is 30Kpa, resulting in smaller deflections of the geosynthetic and smaller surface settlements. Hence these results suggest that the soil suction in the fill enhances the arching behaviour.

This can be seen clearer for the case of a 3m wide void shown in Figure 4.32. This figure shows how the load transfer platform fails when a 3m wide longitudinal void is formed if the suction in the fill is 10 Kpa, but not if it is 30 Kpa. A stable arch cannot clearly be identified when the suction is 30Kpa, but it is clear that the soil suction enhances the load transfer mechanism in the fill preventing it from failing, and allows the load transfer platform to bridge wider voids than when no soil suction was modelled.

This example illustrates the relevance of controlling the compaction properties of the fill embankment during its construction, since the failure of the system may depends upon these properties. On the other hand, taking into account that the levels of soil suction in the fill can change rapidly if the water content of the fill varies, this example also illustrates the danger of assuming that the level of the soil suction remains constant.

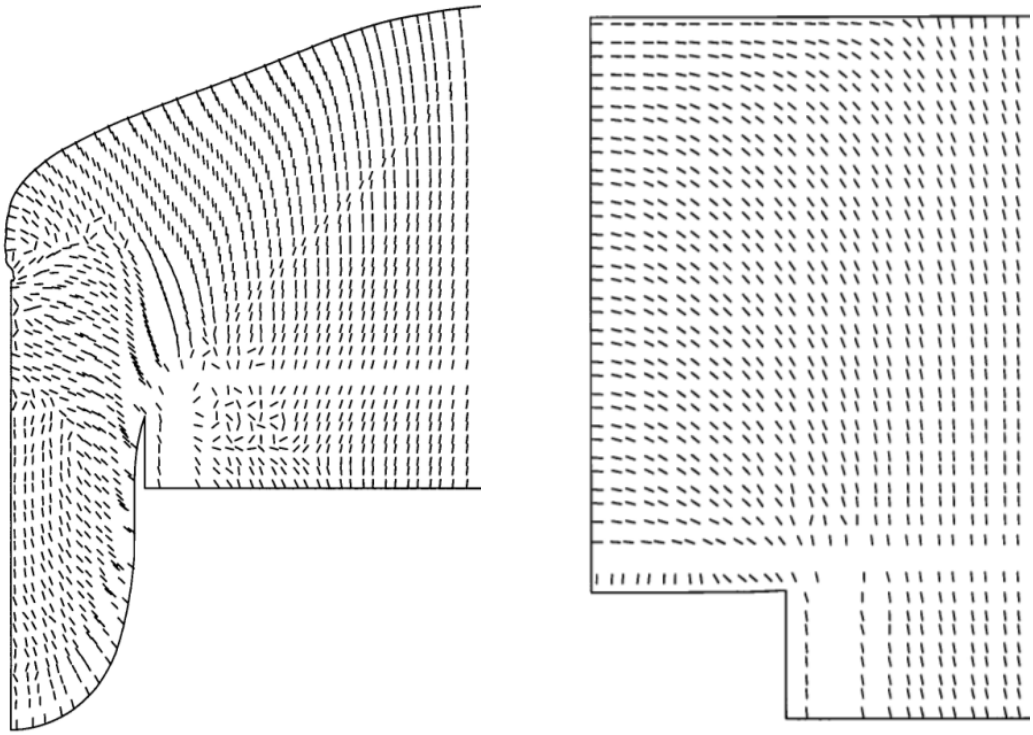

a) Suction = 10Kpa *b) Suction = 30Kpa*

Figure 4.32: Orientation of the major principal stresses above a 3m wide longitudinal void for the 45^0 case and for different values of suction.

In the case when the suction is 10Kpa and the fill collapses into the void it has to be noted that a shear plane rising upwards from the edge of the void with a certain inclination is formed, in the way suggested by Terzaghi's arching theory. When the suction is 30kPa and the load transfer platform is able to bridge the void formed beneath the geosynthetic the orientation of the major principal stresses are closer to those predicted by Hewlett and Randolph's formulation.

The fact that the soil suction in the fill enhances the load transfer mechanism can be further corroborated by considering the geosynthetic deflections above a void of different widths and shapes for different values of the soil suction. The maximum geosynthetic deflections, i.e. the deflection at the centre of the void, above a circular and longitudinal void for the 3 different values of the soil suction in the overlying fill considered and for the case of a 1m and a 2m wide void are shown in Figure 4.33. Figure 4.34 shows the geosynthetics deflections above a 1m void for the case of a circular and a longitudinal void considering the 3 different values of the soil suction.

It can be seen clearly from these figures that the maximum geosynthetic deflections decrease with higher values of the soil suction in the fill for both the circular and longitudinal void and for the 2 void widths considered. This reduction in the geosynthetic deflection is greater for the longitudinal void, since these voids tend to produce greater deflections and stresses at the level of the geosynthetic than the circular voids. The reduction in the vertical displacements of the geosynthetic occurs in all the points directly above the void, as it can be seen in Figure 4.34. The same conclusions can be taken for the rest of the void widths considered in this project, and for both the circular and longitudinal voids.

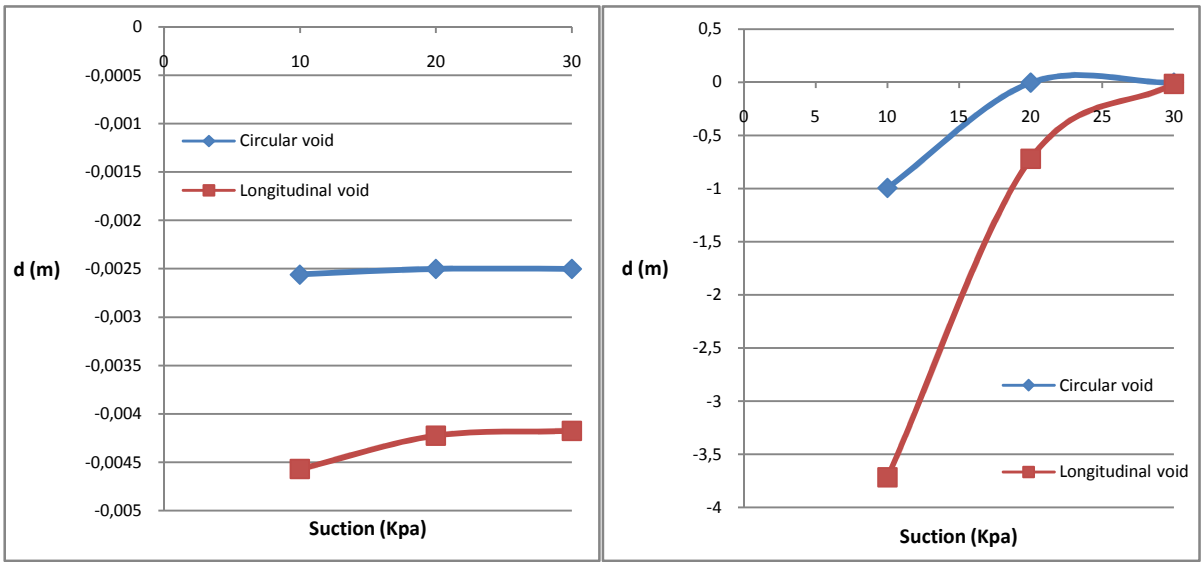

a) D = 1m *b) D = 2m*

Figure 4.33: Maximum geosynthetic deflections above a void of different widths, shapes and for different values of the soil suction

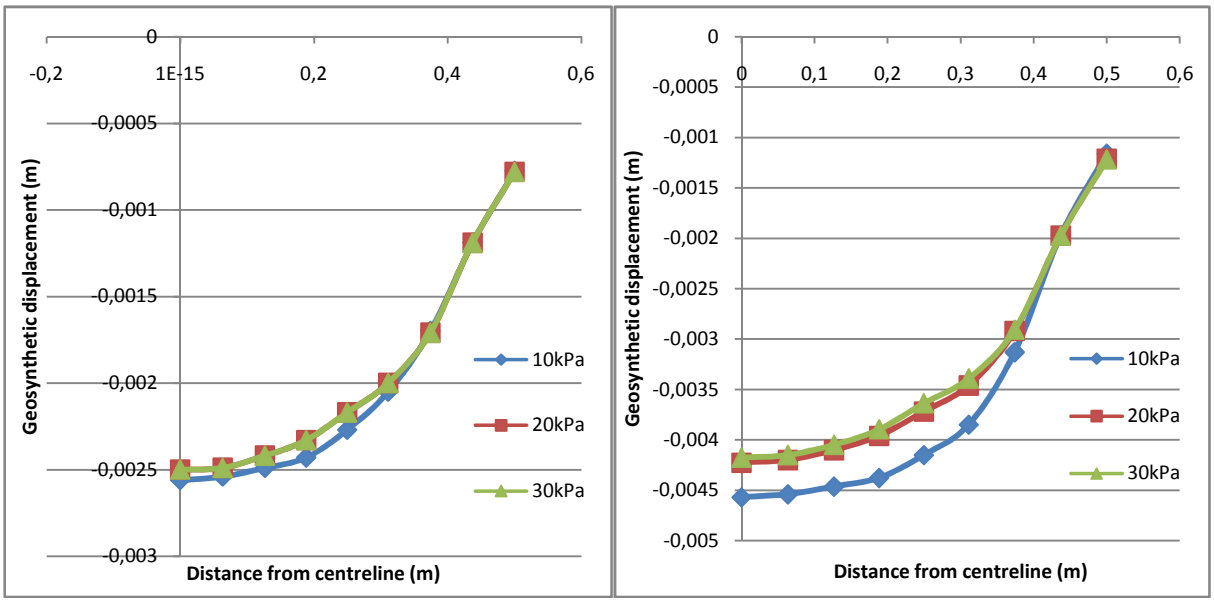

a) Circular void *b) longitudinal void*

Figure 4.34: Geosynthetic deflections above a 1m wide void of different shapes and a varying soil suction with the evolving construction sequence

It can be noted that the reduction in the geosynthetic deflection is almost negligible for the case of a 1m wide void for the two shapes considered. In fact, in the case of a circular void the maximum geosynthetic deflections are identical for the cases in which the soil suction is 20Kpa or 30Kpa. This is due to the fact that a stable soil arch is formed in all three cases, and hence a part of the load of the overlying fill is transferred to the surrounding soil reducing the geosynthetic deflections.

This can be seen graphically in Figure 4.35, which shows the plots of the orientation of the major principal stresses for the three different values of the soil suction. The three plots are almost identical and the same stable arch can be identified.

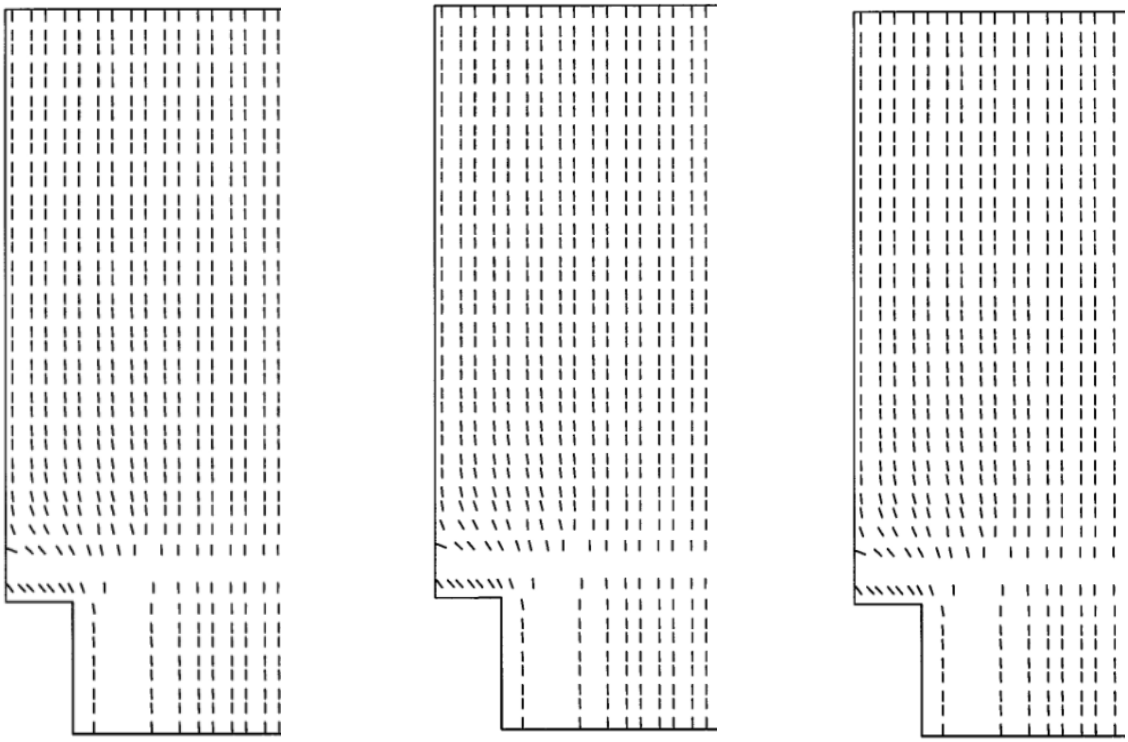

a) Suction = 10Kpa *b) Suction = 20Kpa* *c) Suction = 30Kpa*

Figure 4.35: Orientation of the major principal stresses in the fill above a 1m wide circular void for different values of the soil suction

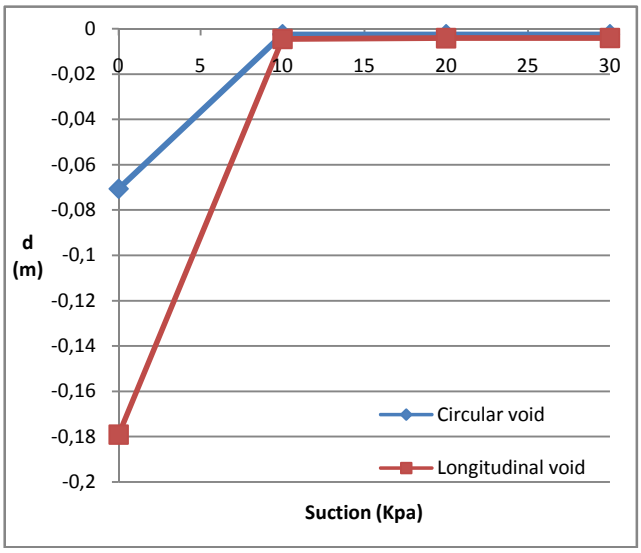

Figure 4.36: Comparison of the maximum geosynthetic deflections above a 1m wide void of different shapes and values of the soil suction with the case in which there is no suction.

Figure 4.35 shows that once a stable arch is formed for a given value of suction, with increasing values of this parameter the same stable arch will be formed, and hence the deflections of the geosynthetic will be the same. The main differences in the geosynthetic deformations occur when the load transfer mechanism does not develop in the fill. For the case of a 1m wide void this happens if there is no suction in the overlying fill. This can be seen clearly in Figure 4.36, where the case of no suction has been included to illustrate this behaviour.

5. Conclusions

The results from the parametric study based in the finite element method performed in order to investigate the mobilisation of the soil arching mechanism with respect to the shape and size of a void forming directly below the geosynthetic in a geosynthetic reinforced load transfer platform have helped to identify some important parameters which affect the behaviour of the whole system.

As previous and wider studies analyzed the case of a vertical sides void, the focus of this study was the effects of the inclination of the vertical sides of the void. Most of the results and conclusions do not differ considerably from the case of a vertical sides void forming beneath the geosynthetic, although some influences of the inclination of the vertical boundaries of the void have been found. The major conclusions that can be drawn from this study are summarised below.

- The two most appropriate arching theories for the case of study are Terzaghi's arching theory and Hewlett & Randolph's formulation. As well as for the vertical sides void case analysed in the literature review, it was found that Terzaghi's arching theory was more generally applicable.

- For the case in which the area of disturbed fill propagated to the surface and hence no stable soil arch was formed it was clear that the vertical stress profile above the centreline of the void predicted by Terzaghi's theory was more accurate that the one predicted with Hewlett & Randolph´s formulation, and that the assumption that the subsiding soil was restricted to the vertical column of soil directly above the void was reasonable.

- In the case in which a stable arch was formed, it was found that Terzaghi's approach was again more suitable in terms of predicting the vertical stress profile above the centreline of the void in the overlying fill, although the orientation of the major principal stresses in the fill could be predicted more accurately using Hewlett & Randolph's formulation. It was also found that the length of the inclined part of the foundation soil can also be adopted as the width of the soil arch proposed in this formulation. This was found to be the major difference between the case of study and the case of a vertical sides void.

- There are no major differences in terms of the deformations and stresses of the geosynthetic or the shape of the deflected geosynthetic between the two different inclinations of the vertical void boundaries studied, for both the cases of a circular or an infinitely long trench.

- The parabolic arc and the circular arcs were both found to be reasonably good approximations for the shape of the deformed geosynthetic above the void, although the circular arc was found to be the best approximation for the shape of the deflected geosynthetic. This represents no difference with the case of a completely vertical boundaries void.

- Increasing the angle of shearing resistance of the overlying fill enhanced the formation of a stable soil arch across the void and hence the stresses and the deflections at the level of the geosynthetic were reduced and wider voids could be bridged.

- The level of soil suction in the overlying fill is seen to have an important influence on the behaviour of the system. The soil suction in the fill enhances the load transfer mechanism and therefore reduced the stresses and deformations of the geosynthetic.

References

Agaiby, S.W., and Jones,C.J.F.P. (1996) Design of reinforced fill systems to support footings overlying cavities. *Geotextiles and Geomembranes,* Elsevier Science Publishers Ltd., England, vol. 14, p.57-727

BS 8006:1995. Code of practice for strengthened/reinforced soils and other fills. British Standards Institution.

Giroud, J.P., Bonaparte, R., Beech, J.F. & Gross, B.A. (1990) *'Design of soil layer-geosynthetic systems overlying voids'*. Geotextiles and Geomembranes, Vol. 9, p11-50

Handy, R.L. (1985) '*The arch in soil arching'*. Journal of the Geotechnical Engineering Division, ASCE, Vol. 111, p302-318.

Hewlett, W.J. & Randolph, M.F. (1988) '*Analysis of piled embankments'*, Ground Engineering, April, p12-18.

Horgan, G.J. & Sarsby, R.W. (2002) '*The arching effect of soils over voids and piles incorporating geosynthetic reinforcement*'. Proceedings of the 7th International Conference on Geosynthetics, Nics, Vol.1, p373-378.

Kempton, G.T., (1992). The use of reinforcement geotextiles to support road embankments over areas subjected to mining subsidence. *Highways and Transportation*, December 1992, pp. 21-31.

Love, J.P. & Milligan, G.W. (2003) 'Design methods for basally reinforced pile-supported emabankments over soft ground'. Ground Engineering, March, p39-43.

Mifsud, A. (2005) '*A parametric study on the behavior of a geosynthetic-reinforced granular fill, as voids develop directly below'*. M.Sc. thesis. Imperial College London

Potts, D.M & Zdravkovic, L.T (1999) '*Finite element analysis in geotechnical engineering: theory'*. Thomas Telford Limited, London.

Potts, D.M & Zdravkovic, L.T (1999) '*Finite element analysis in geotechnical engineering: application'*. Thomas Telford Limited, London.

Potts, V.J (2007) 'Geosynthetic reinforced fill as a load transfer platform to bridge voids'. PhD thesis. Imperial College London.

Russell, D. & Pierpoint, N.D. (1997) 'Recent results in French research on reinforced earth'. Journal of the Construction Division, ASCE, vol.100, p223-237

Shroff, Arvind V. & Shah, Dhananjay L. (2003) '*Soil mechanics and geotechnical engineering*'. Taylor & Francis

Terzaghi, K. (1943) '*Theoretical Soil Mechanics'*. John Wiley & Sons, New York.

Appendix

Appendix 1: Orientation of the major principal stresses and vectors of accumulated displacements in the overlying fill for all the combinations of void width (0.5m, 1m, 2m and 3m) and shape (circular and longitudinal), inclination of the vertical boundaries of the void (45º and 60º) and construction sequence (evolving and existing void).